The interleukin 22 pathway interacts with mutant KRAS to promote poor prognosis in colon cancer

Authors: Sarah McCuaig[1], David Barras[,2], Elizabeth Mann[1], Matthias Friedrich[1], Samuel Bullers[1], Alina Janney[1], Lucy C. Garner[1], Enric Domingo[3], Viktor Hendrik Koelzer[3,4,5], Mauro Delorenzi[2,6,7], Sabine Tejpar[8], Timothy Maughan[9], Nathaniel R. West[1], Fiona Powrie[1]

Affiliations:

[1] Kennedy Institute of Rheumatology, University of Oxford, Oxford UK.

[2] SIB Swiss Institute of Bioinformatics, Bioinformatics Core Facility, Lausanne, Switzerland.

[3]Department of Oncology, University of Oxford, Oxford UK.

[4]Nuffield Department of Medicine, University of Oxford, Oxford UK.

[5]Department of Pathology and Molecular Pathology, University and University Hospital Zurich, Zurich Switzerland.

[6] Ludwig Center for Cancer Research, University of Lausanne, Lausanne, Switzerland.

[7] Department of Oncology, Faculty of Biology and Medicine, University of Lausanne, Lausanne Switzerland.

[8] Molecular Digestive Oncology, KU Leuven, Belgium.

[9] CRUK/MRC Oxford Institute for Radiation Oncology, University of Oxford, Oxford, UK.

Correspondence to: Professor Fiona Powrie; Kennedy Institute of Rheumatology, University of Oxford, Roosevelt Drive, Headington, Oxford, OX3 7YF, UK. Email: fiona.powrie@kennedy.ox.ac.uk

Conflicts of Interest: S.M., N.R.W., and F.P. are inventors on a patent related to IL-22 as a target and prognostic factor in CRC.

Translational Relevance:

IL-22 promotes tumor progression in pre-clinical models of CRC, but its importance in human CRC remains unclear. Using a rigorous discovery/verification analysis of tumor gene expression from over 1,000 patients, we have discovered that among CRC patients with high expression of either or both subunits of the heterodimeric IL-22 receptor, *KRAS* mutation confers poor prognosis. Functional studies revealed that this association is due to an interaction between IL-22 signaling and oncogenic KRAS that enhances tumor cell proliferation through induction of the Myc pathway. These findings demonstrate that cell-intrinsic drivers of CRC can interact with cell-extrinsic factors from the inflammatory microenvironment to influence disease progression. Our data further justify the assessment of *KRAS* mutations in CRC patients, which has until now been clinically beneficial only for prediction of cetuximab responsiveness, and suggest that for *KRAS* mutant CRCs with high IL-22 receptor expression, closer monitoring and more aggressive or alternative therapeutic strategies (e.g. antibody-based blockade of IL-22) could be beneficial.

Abstract:

Purpose: The cytokine interleukin 22 (IL-22) promotes tumor progression in murine models of colorectal cancer (CRC). However, the clinical significance of IL-22 in human CRC remains unclear. We sought to determine whether the IL-22 pathway is associated with prognosis in human CRC, and to identify mechanisms by which IL-22 can influence disease progression.

Experimental Design: Transcriptomic data from stage II/III colon cancers in independent discovery (GSE39582 population-based cohort, N=566) and verification (PETACC3 clinical trial, N=752) datasets were used to investigate the association between IL-22 receptor expression (encoded by the genes *IL22RA1* and *IL10RB*), tumor mutation status, and clinical outcome using Cox proportional hazard models. Functional interactions between IL-22 and mutant KRAS were elucidated using human CRC cell lines and primary tumor organoids.

Results: Transcriptomic analysis revealed a poor-prognosis subset of tumors characterized by high expression of *IL22RA1*, the alpha subunit of the heterodimeric IL-22 receptor, and *KRAS* mutation (RFS: *HR*=2.93, *P*=0.0006; OS: *HR*=2.45, *P*=0.0023). *KRAS* mutations showed a similar interaction with *IL10RB*, and conferred the worst prognosis in tumors with high expression of both *IL22RA1* and *IL10RB* (RFS: *HR*=3.81, *P*=0.0036; OS: *HR*=3.90, *P*=0.0050). Analysis of human CRC cell lines and primary tumor organoids, including an isogenic cell line pair that differed only in *KRAS* mutation status, showed that IL-22 and mutant *KRAS* cooperatively enhance cancer cell proliferation, in part through augmentation of the Myc pathway.

Conclusions: Interactions between *KRAS* and IL-22 signaling may underlie a previously unrecognized subset of clinically aggressive CRC that could benefit from therapeutic modulation of the IL-22 pathway.

Introduction

Colorectal cancer (CRC) is a complex disease driven by the interplay between tumor mutations, environmental factors, and aberrant immunity *(1, 2)*. Chronic intestinal inflammation (e.g. inflammatory bowel disease) is a well-known risk factor for CRC, but colitis-associated cancers account for only a small fraction of total tumor incidence *(3)*. However, CRCs that are not associated with colitis also elicit inflammatory responses, which are thought to be key regulators of tumor progression and therapeutic resistance *(4)*. Indeed, inflammatory cytokines control several key features of malignancy, including cancer cell proliferation, survival, and dissemination *(5)*.

Evidence from preclinical murine models of both sporadic and colitis-associated CRC have implicated interleukin 23 (IL-23) and its downstream effector interleukin 22 (IL-22) in the initiation and progression of colon tumorigenesis *(6–9)*. Furthermore, IL-22 has been associated with human gastric cancer progression *(10)* and has been described to promote CRC stemness *(11)*. IL-23-responsive $CD4^+$ T cells and innate lymphoid cells secrete IL-22 in the tumor microenvironment *(7, 8)*, where it signals through a heterodimeric receptor comprised of IL-10 receptor beta (IL-10RB) and IL-22 receptor alpha 1 (IL-22RA1) *(12)*. In the intestine, IL-22RA1 expression is restricted to the epithelium *(13)* and activates diverse signal transduction pathways in response to IL-22, including JAK/STAT3 (Janus kinase/signal transducer and activator of transcription 3), MAPK (mitogen activated protein kinase), PI3K (phosphatidylinositol-3-kinase), and NF-κB (nuclear factor kappa B), which collectively induce expression of genes involved in cell cycle progression and inhibition of apoptosis *(14–16)*.

Oncogenic Ras isoforms modulate inflammatory pathways in cancer by directly influencing inflammatory cytokine expression and signal transduction *(5)*. IL-23, IL-17, and IL-

22 are elevated in human CRC and their expression is modulated by the presence of mutant Ras *(17)*. Activating mutations in *KRAS*, a major Ras isoform, occur in 40–45% of CRCs and drive constitutive activation of the Ras-Raf-MEK-ERK pathway *(18)*. While KRAS mutations are strongly associated with resistance to EGFR-targeted therapy, they do not correlate with resistance to chemotherapy *(19–21)*. However, given the cytokine-modulating capacity of the Ras family, *KRAS* mutations may be clinically significant in tumors with active cytokine signaling. Oncogenic KRAS could influence virtually all signal transduction pathways downstream of IL-22, but a specific interaction between IL-22 signaling and KRAS mutation has not been described.

In light of the strong evidence pointing toward a pro-tumorigenic role for IL-22 in murine models of CRC, we sought to determine the clinical importance of this cytokine in human disease and to identify subtypes of CRC in which IL-22 signaling may be particularly influential. Our results identify a previously unrecognized interaction between IL-22 signaling and oncogenic KRAS that contributes to tumor cell proliferation and poor patient prognosis.

Materials and Methods

Prognostic study design

Four CRC transcriptomic datasets were analysed in this study (fig. S1A). The French National Cartes d'Identité des Tumeurs (CIT) cohort [GSE39582] *(22)* contains 469 patients with stage II/III CRC who underwent surgery between 1987 and 2007 at seven different centers. Patients who received pre-operative chemotherapy/radiotherapy were excluded from the study. RNA from fresh-frozen primary tumors was assessed using the HG-U133A Affymetrix platform, which contains one probe that detects *IL22RA1* (220056_at).

The Pan-European Trials in Alimentary Tract Cancers (PETACC3) cohort (NCT00026273) was used as a verification set [ArrayExpress:E-MTAB-990]. Data from stage II (n=108) and stage III (n=644) CRC were analyzed *(23, 24)*. Gene expression data were obtained using the ALMAC Colorectal Cancer DSA platform (Craigavon, Northern Ireland), which is a customized Affymetrix chip that includes 61,528 probe sets mapping to 15,920 unique Entrez Gene IDs. The PETACC3 dataset contains three different probes for *IL22RA1*. The probe used in our analysis was that which displayed the greatest variation in the dataset (ADXCRAD_BX089163_s_at). Of note, the second probe was not well-mapped and the third probe had a very narrow dynamic range.

Finally, a merged dataset comprising stage II/III CRC patients of GSE39582 *(22)*, PETACC3 *(23, 24)*, TCGA *(25)*, and ALMAC *(26)*, representing 1,820 patients, was analyzed (referred to in tables as the "Combined" dataset). The ALMAC dataset was obtained from ArrayExpress (www.ebi.ac.uk/arrayexpress) on the A-AFFY-101 platform (customized Affymetrix chip) and is a merge of E-MTAB-863 and E-MTAB-864 *(26)*. Clinical information on overall survival was available for 1,734 patients and on relapse-free survival for 1,499 patients. Gene expression profiles of the patients in the "Combined" dataset were merged at the gene level, then normalized and corrected for batch effects using the *Combat* R package. For the individual analyses of the GSE39582 and PETACC3 datasets, gene expression profiles from each of the datasets were used independently (not normalized to the others). Tumors proximal to the splenic flexure were defined as proximal and tumors distal to the splenic flexure were classified as distal.

All stage II/III patients determined to have a KRAS mutant tumor were included in the analysis. The KRAS mutation sites by codon (where available) are detailed for each of the datasets in fig. S1B.

The interaction between mutant KRAS and all available cytokine/cytokine receptor genes was assessed by Cox proportional hazards tests for interaction using the "Combined" dataset. The top tertile was considered high expression and genes which yielded an uncorrected *P* value of less than 0.05 were considered for further analysis.

Histotype Analysis

Tissue composition of the TCGA and an independent cohort Stratification in COloRecTal cancer (S:CORT) cohorts was assessed by visual pathology review. The S:CORT cohort is composed of 385 FFPE tumors from the FOCUS randomized clinical trial which assessed response to different chemotherapy regimens in patients with advanced CRC *(27)*. H&E slides were scanned at high resolution with an Aperio scanner at a total magnification of 200X. Tissue areas were annotated using the Indica Labs HALO™ digital pathology platform. Small image tiles representing tumor epithelium, desmoplastic stroma, inflamed stroma, mucin and hypocellular stromal areas, necrosis and glass background were generated from >1,500 pathologist-annotated tissue areas. A deep neural network algorithm (Simoyan and Zisserman VGG https://arxiv. org/abs/1409.1556) was trained to segment and quantify individual tissue areas as described in *(28)*. Area measurements were normalized by total stromal content. Tumors were stratified into molecular subgroups based on *IL22RA1* mRNA expression (as described above) and *KRAS* mutation status.

GSEA and CMS Subtype Analysis

Differential expression analysis between *IL22RA1*-high, *KRAS* MUT and *IL22RA1*-high, *KRAS* WT tumors in the Combined dataset was performed using the *limma* R package (version 3.24.4). Using the t-statistics from the differential expression analysis as a weighting factor, a preranked Gene Set Enrichment Analysis (GSEA) using the GenePattern interface from the

Broad Institute (genepattern.broadinstitute.org/) was performed. GSEA was run on MYC_TARGETS_V2 signature from the MSigDB portal (http://www.broadinstitute.org/gsea/msigdb).

Tumors from the Combined dataset were classified according to the "consensus molecular subtypes" (CMS) of colorectal cancer defined by Guinney *et al. (29)*. Tumors were then stratified according to *IL22RA1* and *KRAS* mutation status (as described above). The proportion of tumors in each CMS in the molecular subtypes of interest are displayed.

Colorectal cancer cell lines

The DLD-1 isogenic pair was purchased from Horizon Discovery Group (Parental Line (KRAS G13D): HD PAR-111 Passage 4; Wild type reverted line (KRAS+/-): HD 105-040 Passage 4). Experiments with the isogenic pair were performed between passages 4-9. *KRAS* mutation status in the isogenic pair was confirmed in-house using the qBiomarker^{TM} Somatic Mutation PCR Array Human KRAS Gene (Qiagen, Plate E Format, SMH-806ARE-12 337021). Colo205, SW480, T84, and DLD-1 cells were a generous gift from Dr. Simon Leedham. Colo205 and DLD-1 cells were maintained in RPMI medium (Sigma) with 10% FBS (fetal bovine serum) and 1% P/S (penicillin/streptomycin; Sigma). SW480 cells were cultured in DMEM (Sigma) with 10% FBS and 1% P/S. T84 cells were maintained in DMEM F12 Hams (DMEM Nutrient Mix F-12, D8437, Sigma) with 5% FBS and 1% P/S. Cultures were maintained in 37°C and 5% CO_2. All cell lines were tested for mycoplasma, and determined to be mycoplasma free.

Cytokine stimulation experiments

$3x10^4$ cells per well in 48 well plates were cultured overnight. Cytokines (recombinant human IL-22 [R&D Systems] and recombinant human IL-6 [Peprotech]) were prepared in cell

line-specific media at the concentrations indicated. All cytokine stimulation experiments in the DLD-1 isogenic pair were performed in serum free conditions with 1X ITS (Insulin, Transferrin, Selenium; Sigma). Survival assays confirmed equal viability of both KRAS G13D and KRAS+/- DLD-1 cells in serum free media with 1X ITS.

RNA extraction, cDNA synthesis, and qPCR

RNA was extracted using the Qiagen RNeasy Mini Kit (Qiagen) according to the manufacturer's instructions. cDNA was synthesised using the High Capacity cDNA Kit (Applied Biosystems) according to the manufacturer's protocol using a C1000 Touch^{TM} Thermal Cycler (Bio-Rad). Real-time quantitative polymerase chain reaction (qPCR) analysis was performed using TaqMan Real-Time PCR assays (Life Technologies) and Precision Fast qPCR Mastermix with ROX at a lower level, with inert blue dye (PrimerDesign) and run on a ViiA7 Real-Time PCR System (Applied Biosystems). Data were analysed using the ΔC_T method [$2^{-\Delta CT}$ where $\Delta C_T = C_{T(\text{target gene})} - C_{T(\text{endogenous control})}$]. *RPLPO* was used as the endogenous reference gene for all qPCR analyses.

Immunoblotting

Cells were lysed using a solution of 50mM Tris pH 6.8, 20mM EDTA, 5% SDS, 1mM DTT, and 10% glycerol. Equal protein amounts (15-20µg) were loaded into pre-cast NuPAGE ® Novex 4-12% Bis-Tris Gels (Life Technologies), separated by SDS-PAGE and transferred onto Immobilon-FL PVDF membranes (Millipore). Membranes were blocked (Odyssey ® Blocking Buffer; Li-COR), incubated with primary antibody (total c-Myc [1:1000; Cell Signaling; Clone: D84C12], β actin [1:4000; Sigma; Clone: Ac-74]) overnight at 4°C, and fluorescently conjugated

secondary antibodies (goat anti-rabbit-800CW; 1:15,000; Li-COR; Clone: 925-32211) for 1 hour at room temperature before detection using the Odyssey CLx detection system (Li-COR).

Flow cytometry

For analysis of IL-22RA1 expression, adherent cells were dissociated using TrypLE (Life Technologies), filtered through 70uM filters, and stained with anti-IL-22RA1 (1:10; PE; R&D; Clone 305405) or matched isotype control (1:10; anti-mouse IgG1κ; PE; R&D; Clone 11711), along with anti-EpCAM (1:100; CD326; FITC; Biolegend; Clone 9C4) and a fixable viability dye (1:1000; APC Cy7; eBioscience) for 30 minutes at room temperature before fixation in Fix/Lyse Solution (BD).

For Phosflow experiments, $1x10^6$ cells were stimulated in technical duplicates with 0-100ng/mL IL-22 (R&D Systems) for 30 minutes at 37°C, 5% CO_2. Cells were fixed (Cytofix [BD]) and permeabilized (Perm III Buffer [BD]) according to the manufacturer's protocol and stained for 1 hour at room temperature with fluorescently conjugated antibodies to phosphorylated residues on intracellular signaling proteins of interest (anti-pSTAT3-Y705 [1:10; AF-647; BD; Clone: 4], anti-ERK1/2 (pT202/pY204) [1:10; AF-647; BD; Clone: 20A (RUO)]).

Flow cytometric analysis was performed on an LSR or Fortessa X-20 (BD). Data analysis was performed using FlowJo 10 software (Tree Star).

Proliferation assays

$1x10^4$ cells per well were seeded in 48 well plates and allowed to adhere overnight. Cells were stimulated with 0-200ng/mL IL-22 or IL-6 for 24, 48, and 72h. Cellular viability/proliferation was measured by adding 50μg of MTT to each well 2 hours prior to the end of the IL-22 incubation. At the end of the incubation, supernatants were aspirated, formazan

particles were solubilized with DMSO, and samples transferred to a flat bottom 96 well plate (Costar). Absorbance was measured at 540nm on a BMG SPECTROstar NANO Microplate Reader (BMG Labtech).

siRNA knockdown

$3x10^4$ cells per well in 48 well plates were seeded and allowed to adhere overnight. siRNA was incubated with DharmaFect 2 (Dharmacon) in Opti-MEM (Thermo Fisher) for 20 minutes prior to transfection and cells were transfected using 0.8µL DharmaFect 2 and 40nM ON-TARGET Plus Human MYC SMARTpool (Dharmacon) or ON-TARGET Plus control pool (Dharmacon). Media was replaced with serum free RPMI with 1X ITS (Sigma) after 48h.

Primary CRC whole tissue qPCR analysis and organoid culture

Patients diagnosed with CRC scheduled for colectomy at the Churchill Hospital, Oxford were consented for research use of their resected cancer and matched normal mucosa during a pre-operative appointment. Ethical approval for the study was provided by the National Research Ethics Committees of the UK National Health Service (NHS) in accordance with the Declaration of Helsinki (Reference numbers: 11/YH/0020, 16/YH/0247) under the HTA license 12217. The human samples used in this publication were ethically sourced and their research use was in agreement with the written informed consent. Tumor mutation status was obtained from the Oxford Molecular Diagnostics Centre. Detailed protocols for human organoid culture were generously provided by Marc van de Wetering (Hubrecht Institute, Netherlands). $2mm^3$ fresh CRC biopsies were homogenized using Soft Tissue Homogenizing CK14 Kit vials (Stretton Scientific) in a Precellys 24 (Bertin Instruments) homogeniser (30s at 3500 RPM). RNA extraction, cDNA synthesis, and qPCR analysis were performed as described above.

5-7mm fresh punch biopsies of resected tumor were used to establish organoid cultures as described *(30)*. Genomic DNA was extracted from organoids using the QiaAmp DNA MiniKit (Qiagen) and used for *KRAS* mutation typing. *KRAS* mutation status was determined using the qBiomarker™ Somatic Mutation PCR Array Human KRAS Gene (Qiagen, Plate E Format, SMH-806ARE-12 337021) assay according to the manufacturers protocol. *KRAS* mutation status clinically determined from whole tissue sections, was compared to organoid *KRAS* mutation status to ensure concordance.

For proliferation assays, organoids were dissociated to single cells with TrypLE, re-suspended in reduced growth factor basement membrane extract 2 (BME 2) (Cultrex, Amsbio) and seeded in 5uL BME in 96 well plates. Cells were stimulated with 1ng/mL IL-22 in tumor organoid culture media *(30)*. Media was replaced after 48 hours. 91 hours after initial seeding the media was refreshed again with 1ng/mL IL-22 where appropriate and 10% Alamar Blue (BioRad) and incubated for an additional 5 hours. Absorbance was measured at 570nm and 600nm as a reference on a BMG SPECTROstar NANO Microplate Reader (BMG Labtech). The percent difference in alamar blue reduction for each condition compared to the no treatment condition was determined.

For confocal microscopy, organoids were seeded onto autoclaved 9mm diameter glass coverslips (VWR) in 24 well plates. 400uL of organoid media with 1ng/mL IL-22, as appropriate, was added and organoids were incubated for 30 minutes. Organoids were then fixed on the slides with 4% paraformaldehyde and permeabilised with methanol at -20°C for 10 minutes. Non-specific antibody binding was blocked by incubation with 10% goat serum in TBS and organoids were stained with primary antibody primary antibodies (Phospho-Stat3 (Tyr705) XP Rabbit mAb [1:1000, 9145, clone D3A7, Cell Signaling], anti-E-cadherin [1:300, 610181,

clone 36/E-cadherin, BD]) overnight at 4°C, followed by staining with secondary antibodies (goat anti-rabbit IgG Alexa Fluor 555 [1:400, Life Technologies; A32732] and, goat anti-mouse IgG Alex Fluor 488 [1:400, Life Technologies; A11001]) for 1 hour at room temperature. Nuclei were stained with Hoechst 33258 (1:20,000, Life Technologies) for 10 minutes at room temperature. Coverslips were inverted, and mounted onto Superfrost Plus slides (VWR). Images were acquired on an Olympus FV1200 IX83 Confocal System.

RNA-sequencing

Three independent experiments were performed with DLD-1 isogenic cells at passages 6-8. RNA was extracted following the procedures described above. Library preparation, RNA-sequencing, and quality control were performed by the High-Throughput Genomics Group (Wellcome Trust Centre for Human Genetics, Oxford). Bioanalysis of RNA was performed and all samples had RIN=10. Samples were normalized to 1ug total RNA and the mRNA fraction was isolated by polyA selection. Libraries were prepared using the TruSeq Stranded mRNA Kit (Illumina) and paired-end sequenced using the Illumina HiSeq4000 platform (Illumina). "Strandedness" was tested as part of internal quality control and the proportion of reads mapping to the correct strand was found to be very high. Adapter trimming was performed using cutadapt, alignment was performed using hisat2, indexing was performed with SAMBAMBA, and mapped reads were quantified using featurecounts. Principal component analysis (R package *prcomp* version 3.3.1) was performed on all samples. Pathway analyses were performed by single sample GSEA (ssGSEA) using the GenePattern web interface from the Broad Institute (genepattern.broadinstitute.org/). The Hallmark collection of well-annotated gene sets from the MSigDB portal (http://www.broadinstitute.org/gsea/msigdb) was used. Enrichment scores from ssGSEA were used for differential analysis using the generalized linear model as implemented in

the *limma* package (version 3.30.0). Differentially expressed pathways with an adjusted p-value <0.01 were considered significant. Heat mapping was performed using the *pheatmap* package (version 1.0.8). Sequencing data deposited in NCBI's Gene Expression Omnibus and available through the GEO Series accession number GSE149262.

Statistical analyses

For prognostic studies in tumor transcriptomic datasets all analyses were performed using R software (version 3.03). Receiver operator characteristic (ROC) analysis was performed to determine an optimal *IL22RA1* cutpoint based on log2 expression values in the discovery cohort (GSE39582). The presence or absence of disease relapse at last follow-up was used as the binary variable in this analysis. The *IL22RA1* cutoff value associated with the maximum Youden index (J = sensitivity + specificity −1) was found to be the 67th percentile. This value was used for all subsequent analyses of *IL22RA1* in the discovery and verification datasets, and was also used for analyses of additional cytokine/cytokine receptor genes. Contingency analysis (Fisher's exact test with Bonferroni multiple comparisons correction) was used to assess association of clinicopathological features with *IL22RA1* expression status. Univariate, multivariate, and interaction analyses of relapse-free survival (RFS) and overall survival (OS) were performed using Cox's proportional hazard regression models fitted with the *survival* R package. Interaction analyses were used to assess interactions between *KRAS* mutation status and the expression of cytokine and cytokine receptor genes. Hazard ratios (HRs) were estimated with model coefficients and 95% confidence intervals (CIs) and P values were computed with Wald tests. Time-to-event curves were prepared using Kaplan-Meier methods in GraphPad Prism 7.

For the analysis of *in vitro* experiments in cell lines, and *ex vivo* experiments in primary organoids, all statistical tests were two-sided and are specified in figure legends with exact p-

values displayed. The number of independent experiments performed for each *in vitro* assay is indicated in figure legends. A data point for a given independent experiment is the average of technical replicates (for which 2-3 were performed for each independent experiment). Differences were considered significant when $P<0.05$. All line graphs display mean $\pm$ SEM. For organoid experiments, single dots represent a value from an individual patient (often the average of technical triplicates). Parametric tests were used when $n<8$. These analyses were performed using GraphPad Prism 7.

Results

KRAS mutation is prognostic only in colon cancers that express high amounts of the interleukin 22-receptor gene.

To assess the role of the IL-22 pathway in CRC we first examined expression of *IL22RA1* in stage II/II CRC specimens using transcriptomic data from a publicly available population-based cohort (GSE39582, N=566) *(22)* (fig. S1A). Findings were validated using gene expression data from stage II (N=108) and stage III (N=644) CRC patients enrolled in the PETACC3 (NCT00026273) phase III clinical trial (N=752) *(23, 24)*. Finally, we analyzed a merged dataset comprised of stage II/III CRC patients from GSE39582, PETACC3, and two additional independent cohorts, TCGA and ALMAC (referred to in tables as the "Combined" dataset) (fig. S1A). After excluding patients with missing data or non-stage II/III tumors, 1,083 patients remained for analysis in the Combined dataset (see CONSORT diagram (fig. S1A)). *IL22RA1* was expressed as a continuous variable with a roughly normal distribution (fig. S1C). To determine a cutoff value for classification of *IL22RA1*-high versus low status, we employed ROC statistics and derived the 67th percentile as the cutoff for all subsequent analyses. High *IL22RA1* expression was not significantly associated with patient gender, TNM stage, *KRAS* mutation, or *BRAF* mutation, but was negatively associated with microsatellite instability and proximal tumor location (fig. S1D).

In the GSE39582 discovery cohort, *IL22RA1* expression had no impact on relapse-free survival (RFS) or overall survival (OS) (fig. 1A, fig. S2A). Given that Ras is a mediator of IL-22 signaling, we next stratified patients based on both *IL22RA1* expression and *KRAS* mutation status for further survival analysis. Consistent with prior reports *(21)*, activating *KRAS* mutations were modestly associated with poor clinical outcome (*HR*=1.57, 95% CI=1.11-2.23, *P*=0.0103) (fig. 1B, fig. S2B). However, among cases with high *IL22RA1* expression, *KRAS* mutations were

strongly associated with poor RFS (*HR*=2.93, 95% CI=1.59-5.43, *P*=0.0006) (fig. 1C) and OS (*HR*=2.45, 95% CI=1.38-4.36, *P*=0.0023) (fig. S2C). By contrast, *KRAS* mutations had no prognostic impact in patients with *IL22RA1*-low tumors (RFS *HR*=1.16, 95% CI=0.76-1.78, *P*=0.4840; OS *HR*=1.05, 95% CI=0.69-1.61, *P*=0.813) (fig. 1D, fig. S2D). These findings were validated in the PETACC3 clinical trial cohort (Table 1) and in the large combined cohort (RFS *HR*=2.05, 95% CI=1.45-2.89, *P*<0.0001; OS *HR*=1.65, 95% CI=1.09-2.50, *P*=0.018) (Table 1). Multivariate interaction analysis revealed that the *IL22RA1-KRAS* interaction was independent of tumor site, MSI status, *BRAF* mutation status, and sex (Table 2).

Notably, the prognostic effect of the *IL22RA1-KRAS* interaction was most profound in proximal (right-sided) tumors (RFS, *HR*=4.23, 95% CI=1.38-13.01, *P*=0.012; OS, *HR*=9.41, 95% CI=2.13-41.60, *P*=0.003) (fig. 1EF; Table S1). This observation was independent of microsatellite instability (MSI) and *BRAF* mutation, both of which are common features of proximal tumors (Table S2). Previous studies have demonstrated poor prognosis and response to palliative chemotherapy in advanced CRCs with mucinous histology *(31, 32)*. Given that mucinous adenocarcinoma is associated with proximal tumor location *(33)*, we evaluated differences in the mucinous composition of *IL22RA1*-high proximal versus distal tumors. A histologic analysis was performed on CRC samples from the TCGA and an independent cohort, S:CORT, composed of 385 FFPE tumors from the FOCUS randomized clinical trial which assessed chemotherapy response in patients with advanced CRC *(27)*. There were no differences in the mucinous composition of *IL22RA1*-high distal versus proximal tumors (fig. S3C).

Low immune cell infiltration is a poor prognostic factor for many tumor types, including CRC *(34)*. Since *IL22RA1* is not expressed on hematopoietic cells, high *IL22RA1* expression in specimens analyzed by bulk tumor transcriptomics could be a surrogate for tumors with a paucity of immune infiltrate. In the GSE39582 discovery cohort, *IL22RA1* expression was not correlated

with markers of anti-tumor immunity (*GZMB, IFNG, CD8a*) (fig. S3A). As a control, *IFNG* was compared to *GZMB* and *CD8a* in the cohort. Both comparisons revealed significant correlations, by Pearson correlation analysis (fig. S3A). To better characterize the cellular composition of tumors according to *IL22RA1* and KRAS status, a histologic analysis was performed on CRC samples from the TCGA and S:CORT cohorts. The tumor cell density, inflamed stromal cell density, and non-neoplastic cell count did not differ between the molecular subtypes of interest (fig. S3B). Taken together, these data suggest that *IL22RA1*-high tumors do not simply represent a subset of tumors with low immune infiltrate.

High expression of either or both subunits of the heterodimeric IL-22 receptor confers poor prognosis in KRAS mutant CRC.

Clinical and pre-clinical studies have suggested that several cytokines, including IL-6 and IL-17A, may influence CRC progression *(6, 35–40)*. However, we detected no interaction between *IL6R* (IL-6 receptor) or *IL17RA* (IL-17 receptor) expression (classifying the highest expression tertile for each gene as "high") and *KRAS* mutation status in the combined cohort (Table 2). To determine whether other cytokines and/or their cognate receptors interact with *KRAS* mutation in terms of survival, a Cox proportional hazard interaction analysis was performed on all cytokine and cytokine receptor genes (classifying the highest expression tertile for each gene as "high") and *KRAS* mutation status in the combined cohort. While several cytokine/cytokine receptor genes interacted with *KRAS* mutation, *IL22RA1* displayed the strongest poor-prognosis interaction (fig. 2A). Similarly, *IL10RB*, which encodes the second subunit of the heterodimeric IL-22 receptor, was also a strong interactor (fig. 2A). Detailed survival analysis in the discovery cohort (GSE39582) revealed that like *IL22RA1*-high tumors, *KRAS* mutation was selectively associated with poor prognosis in *IL10RB*-high tumors (RFS,

HR=3.62, 95% CI=1.95-6.70, *P*<0.0001; OS, *HR*=2.43, 95% CI=1.33-4.45, *P*=0.0039; fig. S4); this observation was confirmed in the combined cohort (Table S3).

To determine the effect of high expression of both *IL22RA1* and *IL10RB*, patients were classified into six groups based on *KRAS* mutation status, *IL22RA1,* and *IL10RB*. *KRAS*-mutant tumors with high expression of both cytokine receptor subunits displayed the lowest five-year RFS rates (fig. 2B). In the cohorts analyzed in this study, 18.9% of stage II/III CRCs were *KRAS* mutant and expressed high amounts of *IL22RA1* and/or *IL10RB* compared to 18.8% of CRCs that were *KRAS* mutant and expressed low amounts of both receptors (fig. 2C).

IL-22-induced proliferation of CRC cells is enhanced by KRAS mutation.

IL-22 can promote epithelial proliferation in response to various stimuli *(41–43)*. To investigate a possible functional interaction between IL-22 and mutant *KRAS* we tested the proliferative response of a panel of *KRAS* mutant and wild type CRC cell lines to IL-22. All three cell lines (Colo205 [*KRAS* WT], DLD-1 [*KRAS* MUT], and SW480 [*KRAS* MUT]) were functionally responsive to IL-22, as demonstrated by induction of *SOCS3* (encoding suppressor of cytokine signaling 3) a well-established direct transcriptional target of STAT3 *(44)* (fig. 3A). However, there was no proliferative response to IL-22 in the *KRAS* wild type Colo205 line (fig. 3B). To determine whether proliferative differences were due specifically to the presence or absence of mutant *KRAS,* we employed a DLD-1 isogenic cell line system in which the parental line carries a heterozygous *KRAS* G13D mutation (KRAS-MUT) that was removed to produce paired “wild type” cells (KRAS-WT). IL-22RA1 expression at both the protein (fig. 3C) and mRNA (fig. 3D) level was equivalent in the KRAS-MUT and KRAS-WT isogenic cells, thus providing a pair of cell lines with matched IL-22RA1 expression, differing only in the presence

or absence of mutant *KRAS*. As expected, phosphorylation of ERK1/2 (pERK1/2) was elevated at baseline in the KRAS-MUT cells compared to their KRAS-WT counterparts based on flow cytometry analysis; but pERK1/2 was not induced by IL-22 (fig. 3E). In contrast, IL-22 induced activation of STAT3 (based on flow cytometry analysis of phosphorylation at Y705) in a dose-dependent fashion, but no differences were observed between KRAS-MUT and KRAS-WT cells (fig. 3F). In accordance with the equivalent STAT3 activation in both lines, *SOCS3* induction after IL-22 stimulation was similar in the KRAS-MUT and KRAS-WT cells across a range of IL-22 doses (fig. 3G). Next, we explored whether *KRAS* mutation alters the proliferative response to IL-22. Notably, while IL-22 enhanced proliferation of both KRAS-MUT and KRAS-WT cells, this effect was significantly greater in KRAS-MUT cells (fig. 3H). Like IL-22, IL-6 is a well-known activator of STAT3. However, there was no difference in the proliferative response to IL-6 between KRAS-MUT and WT cells (fig. 3I).

To validate our observations using cells derived from primary tumors, we established organoid cultures from eight freshly resected human CRC samples. Three of these tumors bore oncogenic *KRAS* mutations. IL-22 stimulation induced robust activation of STAT3 in these organoids (fig. 3J). *KRAS* mutant and wild-type organoids were dissociated to single cells and seeded into organoid culture conditions in the presence or absence of 1 ng/mL IL-22 for 96 hours. Consistent with data derived from cell lines, IL-22 significantly increased the viable cell number in cultures of *KRAS*-MUT organoids, but had no consistent effect on *KRAS*-WT organoids (fig. 3K).

Together these data indicate cooperativity between mutant KRAS and IL-22 signaling that promotes the proliferation and accumulation of cancer cells.

Myc is uniquely induced by IL-22 in KRAS mutant cells and promotes cell proliferation

To identify potential modes of interaction between IL-22 and mutant *KRAS*, we next performed unbiased transcriptomic analysis of DLD-1 isogenic cells following IL-22 stimulation. RNA-sequencing was performed on cells stimulated with 10ng/mL IL-22 for 2 hours to identify early transcriptional changes and after 24 hours to explore late changes (fig. 4A). Given that *IL6R* expression does not interact with mutant *KRAS* in a prognostically significant manner (Table 2), nor does it enhance proliferation in *KRAS* mutant versus wild-type cells (fig. 3I), we also stimulated cells with 10ng/mL IL-6 for 2 and 24 hours to identify pathways that are uniquely regulated by IL-22 and not IL-6 (fig. 4A).

Principal component analysis (PCA) revealed that genotype (*KRAS*-MUT or WT), cytokine stimulation (no treatment [NT], IL-22, IL-6), and time (2h, 24h) were the major sources of transcriptomic variation in the dataset (fig. 4B). Gene set enrichment (GSEA) analysis of 24h RNA-seq data revealed that among the Hallmark gene sets (MSigDB), only the Myc pathway ("MYC_TARGETS_V2") was uniquely induced by IL-22 (and not IL-6) in *KRAS*-MUT but not WT cells (fig. 4C). *MYC* expression was significantly increased in *KRAS* mutant versus wild-type cells after 2h IL-22 stimulation (fig. 4D). Although Myc target gene expression was modestly increased by IL-22 in KRAS-MUT cells after 2 hours (fig. S5A), clear preferential induction of Myc targets in KRAS-MUT cells was observed after 24 hours (fig. 4E).

Based on the results of our transcriptomic analyses, we predicted that c-Myc is preferentially induced in *KRAS*-MUT cells following IL-22 stimulation. Indeed, western blot analyses demonstrated a marked time-dependent induction of c-Myc protein in *KRAS*-MUT cells following IL-22 stimulation, whereas c-Myc did not accumulate in *KRAS*-WT cells (fig. 4F, fig. S5B). To determine whether the IL-22-induced proliferation observed in *KRAS*-MUT cells was dependent on c-Myc, we used siRNA to suppress *MYC* expression in DLD-1 *KRAS*-MUT cells,

which reduced c-Myc protein expression by approximately half (fig. S5C). *MYC* knockdown reduced IL-22-induced cell proliferation in DLD-1 *KRAS*-MUT cells (fig. 4G).

Multiple cell types that are not responsive to IL-22 in the tumor microenvironment express *MYC,* complicating the interpretation of *MYC* pathway analysis in whole tumor tissue. Nonetheless, to determine whether the functional differences in *MYC* pathway induction in *IL22RA1*-high, *KRAS*-MUT versus WT cells are reflected in the CRC cohorts assessed in this study, we performed GSEA analysis on transcriptomic data from the combined cohort. The MYC_TARGETS_V2 pathway was not enriched in *IL22RA1*-high, KRAS MUT tumors compared to *IL22RA1*-high, KRAS WT tumors (fig. S6A). However, when tumors in the combined cohort were classified into the CMS subtypes defined by Guinney *et al.* 2015 *(29)*, *IL22RA1* expression was associated with CMS2 status regardless of *KRAS* mutation (fig. S6B). CMS2 is characterized by a molecular signature of epithelial MYC and WNT activation. Moreover, qPCR analysis of *IL22RA1* and *MYC* in prospectively collected whole tumor biopsy tissue from patients undergoing colectomies at the Churchill Hospital, Oxford, revealed that *IL22RA1* positively correlates with *MYC* expression (fig. S6C). *IL22RA1* is not a reported direct transcriptional target of c-Myc. Indeed, *MYC* knockdown in DLD-1 cells did not alter *IL22RA1* expression compared to mock-transfected controls (fig. S6D). Therefore, elevated *MYC* expression in *IL22RA1*-high tumors could be a functional consequence of more active IL-22 signaling.

Discussion

Inflammatory responses are observed in both colitis-associated and sporadic CRC, but whether specific cytokines play beneficial or deleterious roles in cancer is largely context dependent. Moreover, tumors develop adaptations to exploit the growth and survival benefits conferred through cytokine signaling *(5)*. Although data from pre-clinical studies have suggested that IL-22, or its upstream driver cytokine IL-23, may be useful therapeutic targets for CRC, there has been a lack of compelling clinical evidence to support this concept *(6–9, 37, 39, 45, 46)*. Our study extends these previous efforts by demonstrating that IL-22 signaling may be critical for a specific subset of CRC patients, defined by tumors with high IL-22 receptor expression and oncogenic *KRAS* mutations. Furthermore, our data suggest that IL-22 and oncogenic *KRAS* collaborate to promote cell proliferation via enhanced c-Myc activity. These findings emphasize the important and often unpredictable effects that oncogenic mutations can exert on signals derived from the tumor microenvironment.

Prospective analysis of the PETACC3 cohort has previously demonstrated that *KRAS* mutations alone have no prognostic value for stage II/III CRC patients who receive adjuvant chemotherapy *(21)*. Therefore, the negative prognostic effect of *KRAS* mutation in patients with *IL22RA1*-high tumors may be due to a unique interaction between IL-22 signaling and a constitutively active *KRAS* pathway. Notably, in our screen for cytokines and cytokine receptors that interact prognostically with mutant *KRAS*, *IL22RA1* and *IL10RB* (which encode the IL-22 receptor subunits) were the only *KRAS*-interacting genes that showed a significant negative prognostic association. Indeed, despite the well-described tumor-promoting role of IL-6 *(35)*, which is similar to IL-22 in its ability to activate STAT3, neither *IL6* nor *IL6R* expression interacted prognostically with *KRAS*. Intriguingly, high interferon gamma receptor 1 (*IFNGR1*)

expression interacted with *KRAS* and was associated with improved prognosis, which is consistent with the known anti-tumor properties of interferon gamma (IFNγ) *(47)*.

Much of the current understanding of the function and signaling downstream of IL-22 has come from studying its physiologic role in microbial defense and tissue regeneration at barrier surfaces. Due to its anti-apoptotic and mitogenic effects, IL-22 supports intestinal stem cell integrity and tissue regeneration in models of colitis *(48–50)* and graft versus host disease *(43)*. Recent evidence highlights its critical role in regulating DNA damage response pathways in intestinal epithelial stem cells to protect from mutation acquisition and tumor development *(51)*. However, IL-22 can exacerbate immune pathology when produced chronically *(52, 53)*. Based on our data, we propose that IL-22 can also be pathogenic in CRCs with adaptations that alter the functional outcome of IL-22 signaling. In agreement with previously reported findings from Kryczek *et al. (11)*, we found that IL-22 promotes expansion of DLD-1 cells, but only if they expressed constitutively active KRAS. This mutant KRAS-dependent proliferative response to IL-22 was similarly observed in primary CRC organoids.

To date, the only evidence of a potential link between IL-22 signaling and oncogenic *KRAS* is derived from Kras-induced lung cancer models in which genetic ablation of *Il22 (54)* or *Il22ra1 (55)* reduced tumor burden. Moreover, in a small cohort of *KRAS* mutant lung cancer patients (*N*=39), high *IL22RA1* expression conferred poor recurrence-free survival *(54)*. Intriguingly, evidence from a pre-invasive pancreatic neoplasia (PanIN) model revealed that oncogenic *KRAS* and chronic pancreatitis synergistically induce IL-22 and IL-17A production by $CD4^+$ and γδ T cells and that oncogenic *KRAS* augments IL-17 receptor expression on PanIN epithelial cells *(56)*. Based on contingency analyses in the tumor transcriptomic cohorts we studied, mutant *KRAS* and *IL22RA1* expression appear to be independent variables in colon cancer. Consistent with these findings, DLD-1 isogenic cells with or without mutant *KRAS* had

nearly identical IL-22RA1 expression. This suggests that the interaction between *IL22RA1* and mutant *KRAS* is at the level of downstream signaling.

Previous studies of IL-22-driven CRC attributed the pro-tumorigenic activity of IL-22 to its STAT3-activating effect *(7, 8, 11)*. Interestingly, we observed no difference in the amount of IL-22-induced STAT3 activation between *KRAS* mutant and wild type DLD-1 cells. Moreover, the well-described STAT3-activator IL-6 did not augment proliferation in *KRAS* mutant versus wild-type cells, nor did expression of *IL6* or *IL6R* interact with *KRAS* to impact prognosis. Therefore, the interaction between IL-22 and *KRAS* is not due to activation of STAT3 alone. Interestingly, the presence of mutant KRAS enhanced IL-22-induced expression of c-Myc and its downstream target genes. c-Myc is one of the earliest described proto-oncogenes and is a master transcriptional regulator of genes involved in cellular growth, proliferation, metabolism, and biosynthetic processes *(57)*. Notably, the oncogenic activity of c-Myc is largely a consequence of overexpression and, in colorectal cancer, mutations within its coding sequence are very rare *(57)*. Myc expression and stability is regulated at both the transcriptional and post-translational level. STAT3 has been found to augment *MYC* transcription *(58, 59)*, while ERK1/2 and AKT activity downstream of constitutively active Ras signaling enhances c-Myc protein stability and extends its half-life *(60, 61)*; both mechanisms could be at play in IL-22-induced c-Myc in *KRAS* mutant cells.

Based on the evidence presented here, we propose a stratification strategy in which tumors from CRC patients are subjected to standard *KRAS* mutation typing paired with quantification of IL-22 receptor expression. Although both IL-22RA1 and IL-10RB contribute prognostic information, IL-22RA1 expression is restricted to epithelial cells in the colon and may thus be a more suitable biomarker. CRCs harboring *KRAS* mutations and high expression of *IL22RA1* and/or *IL10RB* comprise approximately 19% of the total CRC population. Such

patients are predicted to have lower responsiveness to conventional chemotherapy, increased frequency of disease relapse, and reduced overall survival time. Beyond prognostic stratification, our data suggest that pharmacological blockade of IL-22 signaling may be therapeutically beneficial for KRAS-mutant tumors. Notably, monoclonal antibodies targeting IL-22 and its upstream driver IL-23 have been developed for inflammatory indications and were well tolerated in Phase I and II studies (NCT00563524, NCT00883896, NCT01866007, NCT02203032, NCT01225731). Furthermore, antibodies specific to the p19 subunit of IL-23 are now being investigated in Phase II/III trials in inflammatory bowel disease (NCT03926130, NCT03466411, NCT03759288, NCT03398135) and will provide gut-specific safety and efficacy data.

Although we have revealed a novel interaction between KRAS and IL-22 in CRC, several questions remain. For example, our analyses focused on the direct effect of IL-22 on cancer-cell intrinsic pathways, but whether IL-22 differentially affects the tumor microenvironment based on KRAS mutation status is unknown. In addition, our cohorts were not sufficiently powered to study whether IL-22 signaling interacts with constitutively active BRAF, an immediate downstream mediator of Ras signaling that is mutated in approximately 10% of CRCs. Because *IL22RA1* expression manifests as a continuous, non-biphasic variable, further prospective studies assessing *IL22RA1* expression are necessary (and ongoing in our laboratory) to establish a clinically relevant cut-point for identifying patients with high expression.

Collectively, the evidence presented here suggests a method to both identify a subset of poor prognosis CRC patients with *KRAS* mutant tumors and to target these tumors using therapeutic blockade of the IL-22 pathway. Interactions between cytokines and oncogenic mutations are not limited to IL-22 and *KRAS*. Exploration and exploitation of cytokine-oncogene interactions more broadly may be beneficial for precise patient stratification and the application of immunomodulatory therapies in cancer.

Authors' Contributions

Conception and design: S.M., N.R.W., F.P., T.M.

Development of methodology: S.M., N.R.W., D. B., F. P., T.M.

Acquisition of data (provided animals, acquired and managed patients, provided facilities, etc.): S.M., D.B., E.M., M.F., S.B., A.J., L.G., E.D., V.H.K., Oxford IBD Cohort Investigators, S.T., M.D., T.M., N.R.W., F.P.

Analysis and interpretation of data (e.g., statistical analysis, biostatistics, computational analysis): S.M., D.B., E.M., M.D., N.R.W., F.P., T.M.

Writing, review, and/or revision of the manuscript: S.M., N.R.W., E.M., F.P. and all authors provided comments.

Administrative, technical, or material support (i.e., reporting or organizing data, constructing databases): D.B., S.B., M.D.

Acknowledgements:

We thank the Oxford IBD Cohort Investigators[1] for helping to facilitate and coordinate GI specimen collection. Thank you to Cloe Vassart, James Chivenga, Ngonidzashe Charumbira, and David Maldonado-Perez who consented patients and collected samples from the operating theatres for this study. We thank the team of pathologists at the JR Hospital for biopsying specimens and S. Page in the Oxford Molecular Diagnostics Centre for providing tumor mutation status data. We thank Dr. Simon Leedham for generously providing cell lines and Dr. Marc Van de Wetering of the Hubrecht Institue, Utrecht for providing human organoid protocols. We thank the High-Throughput Genomics Group at the Wellcome Trust Centre for Human Genetics (funded by Wellcome Trust grant reference 090532/Z/09/Z) for generation of the RNA-sequencing data and Nicholas Illott for assisting with NCBI GEO data deposition. We thank the patients and their families for contributing to this study.

This work was funded by an Oxford/CRUK Development Fund Grant (C25255/A18085) and an MRC Experimental Medicine Grant (MR/N02690X/1). S. M. was supported by the Rhodes Trust. N.R.W. was supported by an Irivington Institute Postdoctoral Fellowship (Cancer Research Institute). L.G. is supported by a Wellcome Trust PhD Studentship (109028/Z/15/Z). E.D. is supported by the S:CORT Consortium which is funded by a grant from the Medical Research Council and Cancer Research UK. This work was also supported by the NIHR Oxford Biomedical Research Centre. The views expressed are those of the authors and not necessarily those of the NHS, the NIHR or the Department of Health.

[1] Carolina V. Arancibia-Cárcamo; Adam Bailey; Ellie Barnes; Elizabeth Bird-Lieberman; Oliver Brain; Barbara Braden; Jane Collier; James East; Alessandra Geremia; Lucy Howarth; Satish Keshav; Paul Klenerman; Simon Leedham; Rebecca Palmer; Fiona Powrie; Astor Rodrigues; Jack Satsangi; Alison Simmons; Peter Sullivan; Simon Travis; Holm Uhlig

References:

1. J. Terzić, S. Grivennikov, E. Karin, M. Karin, Inflammation and colon cancer., *Gastroenterology* **138**, 2101-2114.e5 (2010).

2. E. Elinav, R. Nowarski, C. a Thaiss, B. Hu, C. Jin, R. a Flavell, Inflammation-induced cancer: crosstalk between tumours, immune cells and microorganisms., *Nat. Rev. Cancer* **13**, 759–71 (2013).

3. T. Jess, C. Rungoe, L. Peyrin–Biroulet, Risk of Colorectal Cancer in Patients With Ulcerative Colitis: A Meta-analysis of Population-Based Cohort Studies, *Clin. Gastroenterol. Hepatol.* **10**, 639–645 (2012).

4. D. Hanahan, R. a Weinberg, Hallmarks of cancer: the next generation., *Cell* **144**, 646–74 (2011).

5. N. R. West, S. McCuaig, F. Franchini, F. Powrie, Emerging cytokine networks in colorectal cancer, *Nat. Rev. Immunol.* **15**, 615–629 (2015).

6. S. Grivennikov, K. Wang, D. Mucida, C. A. Stewart, B. Schnabl, D. Jauch, K. Taniguchi, G.-Y. Yu, C. H. Osterreicher, K. E. Hung, C. Datz, Y. Feng, E. R. Fearon, M. Oukka, L. Tessarollo, V. Coppola, F. Yarovinsky, H. Cheroutre, L. Eckmann, G. Trinchieri, M. Karin, Adenoma-linked barrier defects and microbial products drive IL-23/IL-17-mediated tumour growth., *Nature* **491**, 254–8 (2012).

7. S. Huber, N. Gagliani, L. a Zenewicz, F. J. Huber, L. Bosurgi, B. Hu, M. Hedl, W. Zhang, W. O'Connor, A. J. Murphy, D. M. Valenzuela, G. D. Yancopoulos, C. J. Booth, J. H. Cho, W. Ouyang, C. Abraham, R. A. Flavell, IL-22BP is regulated by the inflammasome and modulates tumorigenesis in the intestine., *Nature* **491**, 259–63 (2012).

8. S. Kirchberger, D. J. Royston, O. Boulard, E. Thornton, F. Franchini, R. L. Szabady, O. Harrison, F. Powrie, Innate lymphoid cells sustain colon cancer through production of interleukin-22 in a mouse model, *J. Exp. Med.* **210**, 917–931 (2013).

9. C. Wang, G. Gong, A. Sheh, S. Muthupalani, E. M. Bryant, D. A. Puglisi, H. Holcombe, E. A. Conaway, N. A. P. Parry, V. Bakthavatchalu, S. P. Short, C. S. Williams, G. N. Wogan, S. R. Tannenbaum, J. G. Fox, B. H. Horwitz, Interleukin-22 drives nitric oxide-dependent DNA damage and dysplasia in a murine model of colitis-associated cancer, *Mucosal Immunol.* , 1–14 (2017).

10. Y. Zhuang, L.-S. Peng, Y.-L. Zhao, Y. Shi, X.-H. Mao, G. Guo, W. Chen, X.-F. Liu, J.-Y. Zhang, T. Liu, P. Luo, P.-W. Yu, Q.-M. Zou, Increased intratumoral IL-22-producing CD4(+) T cells and Th22 cells correlate with gastric cancer progression and predict poor patient survival., *Cancer Immunol. Immunother.* **61**, 1965–75 (2012).

11. I. Kryczek, Y. Lin, N. Nagarsheth, D. Peng, L. Zhao, E. Zhao, L. Vatan, W. Szeliga, Y. Dou, S. Owens, W. Zgodzinski, M. Majewski, G. Wallner, J. Fang, E. Huang, W. Zou, IL-22(+)CD4(+) T cells promote colorectal cancer stemness via STAT3 transcription factor activation and induction of the methyltransferase DOT1L., *Immunity* **40**, 772–784 (2014).

12. A. L. Gurney, IL-22, a Th1 cytokine that targets the pancreas and select other peripheral tissues., *Int. Immunopharmacol.* **4**, 669–77 (2004).

13. Y. Zheng, P. a Valdez, D. M. Danilenko, Y. Hu, S. M. Sa, Q. Gong, A. R. Abbas, Z.

Modrusan, N. Ghilardi, F. J. de Sauvage, W. Ouyang, Interleukin-22 mediates early host defense against attaching and effacing bacterial pathogens, *Nat. Med.* **14**, 282–289 (2008).

14. A. Mitra, S. K. Raychaudhuri, S. P. Raychaudhuri, IL-22 induced cell proliferation is regulated by PI3K/Akt/mTOR signaling cascade., *Cytokine* **60**, 38–42 (2012).

15. M.-J. Xu, D. Feng, H. Wang, Y. Guan, X. Yan, B. Gao, IL-22 ameliorates renal ischemia-reperfusion injury by targeting proximal tubule epithelium., *J. Am. Soc. Nephrol.* **25**, 967–77 (2014).

16. C. Lim, R. Savan, The role of the IL-22/IL-22R1 axis in cancer., *Cytokine Growth Factor Rev.* **25**, 257–71 (2014).

17. S. Petanidis, D. Anestakis, M. Argyraki, M. Hadzopoulou-Cladaras, A. Salifoglou, Differential expression of IL-17, 22 and 23 in the progression of colorectal cancer in patients with K-ras mutation: Ras signal inhibition and crosstalk with GM-CSF and IFN-γ., *PLoS One* **8**, e73616 (2013).

18. F. Sinicrope, Q. Shi, T. C. Smyrk, S. N. Thibodeau, R. Dienstmann, J. Guinney, B. M. Bot, S. Tejpar, M. Delorenzi, R. M. Goldberg, M. Mahoney, D. J. Sargent, S. R. Alberts, Molecular Markers Identify Subtypes of Stage III Colon Cancer Associated With Patient Outcomes., *Gastroenterology* **148**, 88–99 (2014).

19. C. Karapetis, S. Khambata-Ford, D. Jonker, C. O'Callaghan, D. Tu, N. Tebbutt, K-ras Mutations and Benefit from Cetuximab in Advanced Colorectal Cancer, *N. Engl. J. Med.* **359**, 1757–1765 (2008).

20. E. Van Cutsem, H.-J. Lenz, C.-H. Kohne, V. Heinemann, S. Tejpar, I. Melezinek, F. Beier, C. Stroh, P. Rougier, J. H. van Krieken, F. Ciardiello, Fluorouracil, Leucovorin, and Irinotecan Plus Cetuximab Treatment and RAS Mutations in Colorectal Cancer, *J. Clin. Oncol.* **33**, 692–700 (2015).

21. A. D. Roth, S. Tejpar, M. Delorenzi, P. Yan, R. Fiocca, D. Klingbiel, D. Dietrich, B. Biesmans, G. Bodoky, C. Barone, E. Aranda, B. Nordlinger, L. Cisar, R. Labianca, D. Cunningham, E. Van Cutsem, F. Bosman, Prognostic Role of KRAS and BRAF in Stage II and III Resected Colon Cancer: Results of the Translational Study on the PETACC-3, EORTC 40993, SAKK 60-00 Trial, *J. Clin. Oncol.* **28**, 466–474 (2010).

22. L. Marisa, A. de Reyniès, A. Duval, J. Selves, M. P. Gaub, L. Vescovo, M.-C. Etienne-Grimaldi, R. Schiappa, D. Guenot, M. Ayadi, S. Kirzin, M. Chazal, J.-F. Fléjou, D. Benchimol, A. Berger, A. Lagarde, E. Pencreach, F. Piard, D. Elias, Y. Parc, S. Olschwang, G. Milano, P. Laurent-Puig, V. Boige, Gene expression classification of colon cancer into molecular subtypes: characterization, validation, and prognostic value., *PLoS Med.* **10**, e1001453 (2013).

23. V. Popovici, E. Budinska, S. Tejpar, S. Weinrich, H. Estrella, G. Hodgson, E. Van Cutsem, T. Xie, F. T. Bosman, A. D. Roth, M. Delorenzi, Identification of a poor-prognosis BRAF-mutant - Like population of patients with colon cancer, *J. Clin. Oncol.* **30**, 1288–1295 (2012).

24. A. D. Roth, M. Delorenzi, S. Tejpar, P. Yan, D. Klingbiel, R. Fiocca, G. D'Ario, L. Cisar, R. Labianca, D. Cunningham, B. Nordlinger, F. Bosman, E. Van Cutsem, Integrated analysis of molecular and clinical prognostic factors in stage II/III colon cancer, *J. Natl. Cancer Inst.* **104**, 1635–1646 (2012).

25. Cancer Genome Atlas Network, D. M. Muzny, Comprehensive molecular characterization of human colon and rectal cancer, *Nature* **487**, 330–337 (2012).

26. R. D. Kennedy, M. Bylesjo, P. Kerr, T. Davison, J. M. Black, E. W. Kay, R. J. Holt, V. Proutski, M. Ahdesmaki, V. Farztdinov, N. Goffard, P. Hey, F. McDyer, K. Mulligan, J. Mussen, E. O'Brien, G. Oliver, S. M. Walker, J. M. Mulligan, C. Wilson, A. Winter, D. O'Donoghue, H. Mulcahy, J. O'Sullivan, K. Sheahan, J. Hyland, R. Dhir, O. F. Bathe, O. Winqvist, U. Manne, C. Shanmugam, S. Ramaswamy, E. J. Leon, W. I. Smith, U. McDermott, R. H. Wilson, D. Longley, J. Marshall, R. Cummins, D. J. Sargent, P. G. Johnston, D. P. Harkin, Development and independent validation of a prognostic assay for stage ii colon cancer using formalin-fixed paraffin-embedded tissue, *J. Clin. Oncol.* **29**, 4620–4626 (2011).

27. M. T. Seymour, T. S. Maughan, J. A. Ledermann, C. Topham, R. James, S. J. Gwyther, D. B. Smith, S. Shepherd, A. Maraveyas, D. R. Ferry, A. M. Meade, L. Thompson, G. O. Griffiths, M. K. Parmar, R. J. Stephens, Different strategies of sequential and combination chemotherapy for patients with poor prognosis advanced colorectal cancer (MRC FOCUS): a randomised controlled trial, *Lancet* **370**, 143–152 (2007).

28. E. Domingo, A. Chatzipli, S. Richman, A. Blake, C. Hardy, C. Whalley, K. Redmon, I. Tomlinson, P. Dunne, S. Walker, A. Beggs, U. McDermott, G. I. Murray, L. M. Samuel, M. Seymour, P. Quirke, T. Maughan, V. H. Koelzer, Abstract 4446: Assessment of tissue composition with digital pathology in colorectal cancer, *Cancer Res.* **79**, 4446 LP – 4446 (2019).

29. J. Guinney, R. Dienstmann, X. Wang, A. de Reyniès, A. Schlicker, C. Soneson, L. Marisa, P. Roepman, G. Nyamundanda, P. Angelino, B. M. Bot, J. S. Morris, I. M. Simon, S. Gerster, E. Fessler, F. De Sousa E Melo, E. Missiaglia, H. Ramay, D. Barras, K. Homicsko, D. Maru, G. C. Manyam, B. Broom, V. Boige, B. Perez-Villamil, T. Laderas, R. Salazar, J. W. Gray, D. Hanahan, J. Tabernero, R. Bernards, S. H. Friend, P. Laurent-Puig, J. P. Medema, A. Sadanandam, L. Wessels, M. Delorenzi, S. Kopetz, L. Vermeulen, S. Tejpar, The consensus molecular subtypes of colorectal cancer, *Nat. Med.* **21**, 1350–1356 (2015).

30. M. van de Wetering, H. E. Francies, J. M. Francis, G. Bounova, F. Iorio, A. Pronk, W. van Houdt, J. van Gorp, A. Taylor-Weiner, L. Kester, A. McLaren-Douglas, J. Blokker, S. Jaksani, S. Bartfeld, R. Volckman, P. van Sluis, V. S. W. Li, S. Seepo, C. Sekhar Pedamallu, K. Cibulskis, S. L. Carter, A. McKenna, M. S. Lawrence, L. Lichtenstein, C. Stewart, J. Koster, R. Versteeg, A. van Oudenaarden, J. Saez-Rodriguez, R. G. J. Vries, G. Getz, L. Wessels, M. R. Stratton, U. McDermott, M. Meyerson, M. J. Garnett, H. Clevers, Prospective Derivation of a Living Organoid Biobank of Colorectal Cancer Patients, *Cell* **161**, 933–945 (2015).

31. D. Lee, S. Han, H. J. Lee, Y. Rhee, J. M. Bae, N. Cho, K. Lee, T. Kim, D. Oh, S. Im, Y. Bang, S. Jeong, K. J. Park, J. Park, G. H. Kang, T. Kim, Prognostic implication of mucinous histology in colorectal cancer patients treated with adjuvant FOLFOX chemotherapy, **108**, 1978–1984 (2013).

32. F. Negri, A. De Giorgi, A. Gilli, C. Azzoni, L. Bottarelli, L. Gnetti, M. Goldoni, L. Manotti, P. Sgargi, M. Michiara, F. Leonardi, G. Rindi, S. Cascinu, E. M. Silini, Impact of laterality and mucinous histology on relapse-free and overall survival in a registry-based colon cancer series, *Sci. Rep.* **9**, 1–9 (2019).

33. S. Leopoldo, B. Lorena, A. Cinzia, D. C. Gabriella, B. A. Luciana, C. Renato, M. Antonio, S. Carlo, P. Cristina, C. Stefano, T. Maurizio, R. Luigi, B. Cesare, Two Subtypes of Mucinous Adenocarcinoma of The Colorectum : Clinicopathological and Genetic Features, *Ann. Surg. Oncol.* **15**, 1429–1439 (2008).

34. T. A. Barnes, E. Amir, HYPE or HOPE : the prognostic value of infiltrating immune cells in cancer, *Br. J. Cancer* **117**, 451–460 (2017).

35. J. Bollrath, T. J. Phesse, V. a von Burstin, T. Putoczki, M. Bennecke, T. Bateman, T. Nebelsiek, T. Lundgren-May, O. Canli, S. Schwitalla, V. Matthews, R. M. Schmid, T. Kirchner, M. C. Arkan, M. Ernst, F. R. Greten, gp130-mediated Stat3 activation in enterocytes regulates cell survival and cell-cycle progression during colitis-associated tumorigenesis., *Cancer Cell* **15**, 91–102 (2009).

36. S. Grivennikov, E. Karin, J. Terzic, D. Mucida, G.-Y. Yu, S. Vallabhapurapu, J. Scheller, S. Rose-John, H. Cheroutre, L. Eckmann, M. Karin, IL-6 and Stat3 Are Required for Survival of Intestinal Epithelial Cells and Development of Colitis-Associated Cancer, *Cancer Cell* **15**, 103–113 (2009).

37. S. Wu, K.-J. Rhee, E. Albesiano, S. Rabizadeh, X. Wu, H. Yen, D. L. Huso, F. L. Brancati, E. Wick, F. McAllister, F. Housseau, D. M. Pardoll, C. L. Sears, A human colonic commensal promotes colon tumorigenesis via activation of T helper type 17 T cell responses, *Nat. Med.* **15**, 1016–1022 (2009).

38. W.-J. Chae, T. F. Gibson, D. Zelterman, L. Hao, O. Henegariu, A. L. M. Bothwell, Ablation of IL-17A abrogates progression of spontaneous intestinal tumorigenesis, *Proc. Natl. Acad. Sci.* **107**, 5540–5544 (2010).

39. K. Wang, M. K. Kim, G. Di Caro, J. Wong, S. Shalapour, J. Wan, W. Zhang, Z. Zhong, E. Sanchez-Lopez, L.-W. Wu, K. Taniguchi, Y. Feng, E. Fearon, S. Grivennikov, M. Karin, Interleukin-17 receptor A signaling in transformed enterocytes promotes early colorectal tumorigenesis, *Immunity* **41**, 1052–1063 (2014).

40. M. Tosolini, A. Kirilovsky, B. Mlecnik, T. Fredriksen, S. Mauger, G. Bindea, A. Berger, P. Bruneval, W.-H. Fridman, F. Pagès, J. Galon, Clinical impact of different classes of infiltrating T cytotoxic and helper cells (Th1, Th2, Treg, Th17) in patients with colorectal cancer., *Cancer Res.* **71**, 1263–71 (2011).

41. S. J. Aujla, Y. R. Chan, M. Zheng, M. Fei, D. J. Askew, D. A. Pociask, T. A. Reinhart, F. McAllister, J. Edeal, K. Gaus, S. Husain, J. L. Kreindler, P. J. Dubin, J. M. Pilewski, M. M. Myerburg, C. A. Mason, Y. Iwakura, J. K. Kolls, IL-22 mediates mucosal host defense against Gram-negative bacterial pneumonia, *Nat. Med.* **14**, 275–81 (2008).

42. S. Eyerich, C. B. Schmidt-Weber, S. Eyerich, K. Eyerich, D. Pennino, T. Carbone, F. Nasorri, S. Pallotta, F. Cianfarani, T. Odorisio, C. Traidl-hoffmann, H. Behrendt, S. R. Durham, C. B. Schmidt-weber, A. Cavani, Th22 cells represent a distinct human T cell subset involved in epidermal immunity and remodeling, *J. Clin. Invest.* **119**, 3573–3585 (2009).

43. C. A. Lindemans, M. Calafiore, A. M. Mertelsmann, M. H. O'Connor, J. A. Dudakov, R. R. Jenq, E. Velardi, L. F. Young, O. M. Smith, G. Lawrence, J. A. Ivanov, Y.-Y. Fu, S. Takashima, G. Hua, M. L. Martin, K. P. O'Rourke, Y.-H. Lo, M. Mokry, M. Romera-Hernandez, T. Cupedo, L. E. Dow, E. E. Nieuwenhuis, N. F. Shroyer, C. Liu, R. Kolesnick, M. R. M. van den Brink, A. M. Hanash, Interleukin-22 promotes intestinal-stem-cell-mediated epithelial regeneration, *Nature* **528**, 560–564 (2015).

44. M. L. Nagalakshmi, A. Rascle, S. Zurawski, S. Menon, R. de Waal Malefyt, Interleukin-22 activates STAT3 and induces IL-10 by colon epithelial cells., *Int. Immunopharmacol.* **4**, 679–91 (2004).

45. J. L. Langowski, X. Zhang, L. Wu, J. D. Mattson, T. Chen, K. Smith, B. Basham, T. McClanahan, R. a Kastelein, M. Oft, IL-23 promotes tumour incidence and growth., *Nature* **442**, 461–5 (2006).

46. Y. S. Hyun, D. S. Han, A. R. Lee, C. S. Eun, J. Youn, H.-Y. Kim, Role of IL-17A in the development of colitis-associated cancer, *Carcinogenesis* **33**, 931–936 (2012).

47. H. Ikeda, L. J. Old, R. D. Schreiber, The roles of IFNy in protection against tumor development and cancer immunoediting, *Cytokine Growth Factor Rev.* **13**, 95–109 (2002).

48. K. Sugimoto, A. Ogawa, E. Mizoguchi, Y. Shimomura, A. Andoh, A. K. Bhan, R. S. Blumberg, R. J. Xavier, A. Mizoguchi, IL-22 ameliorates intestinal inflammation in a mouse model of ulcerative colitis, *J. Clin. Invest.* **118**, 534–44 (2008).

49. L. a Zenewicz, G. D. Yancopoulos, D. M. Valenzuela, A. J. Murphy, S. Stevens, R. a Flavell, Innate and Adaptive Interleukin-22 Protects Mice from Inflammatory Bowel Disease, *Immunity* **29**, 947–957 (2008).

50. C. L. Zindl, J.-F. Lai, Y. K. Lee, C. L. Maynard, S. N. Harbour, W. Ouyang, D. D. Chaplin, C. T. Weaver, IL-22-producing neutrophils contribute to antimicrobial defense and restitution of colonic epithelial integrity during colitis, *Proc. Natl. Acad. Sci.* **110**, 12768–12773 (2013).

51. K. Gronke, P. P. Hernández, J. Zimmermann, C. S. N. Klose, M. Kofoed-Branzk, F. Guendel, M. Witkowski, C. Tizian, L. Amann, F. Schumacher, H. Glatt, A. Triantafyllopoulou, A. Diefenbach, Interleukin-22 protects intestinal stem cells against genotoxic stress., *Nature* **566**, 249–253 (2019).

52. H. Ma, S. Liang, J. Li, L. Napierata, T. Brown, S. Benoit, M. Senices, D. Gill, K. Dunussi-Joannopoulos, M. Collins, C. Nickerson-Nutter, L. a Fouser, D. a Young, IL-22 is required for Th17 cell–mediated pathology in a mouse model of psoriasis-like skin inflammation, *J. Clin. Invest.* **118**, 597–607 (2008).

53. M. Muñoz, M. M. Heimesaat, K. Danker, D. Struck, U. Lohmann, R. Plickert, S. Bereswill, A. Fischer, I. R. Dunay, K. Wolk, C. Loddenkemper, H.-W. Krell, C. Libert, L. R. Lund, O. Frey, C. Hölscher, Y. Iwakura, N. Ghilardi, W. Ouyang, T. Kamradt, R. Sabat, O. Liesenfeld, Interleukin (IL)-23 mediates Toxoplasma gondii –induced immunopathology in the gut via matrixmetalloproteinase-2 and IL-22 but independent of IL-17, *J. Exp. Med.* **206**, 3047–3059 (2009).

54. N. Khosravi, M. S. Caetano, A. M. Cumpian, N. Unver, C. De la Garza Ramos, O. Noble, S. Daliri, B. J. Hernandez, B. A. Gutierrez, S. E. Evans, S. Hanash, A. M. Alekseev, Y. Yang, S. H. Chang, R. Nurieva, H. Kadara, J. Chen, E. J. Ostrin, S. J. Moghaddam, IL22 Promotes Kras Mutant Lung Cancer by Induction of a Pro-Tumor Immune Response and Protection of Stemness Properties., *Cancer Immunol. Res.* **6**, canimm.0655.2017 (2018).

55. C. Jin, G. K. Lagoudas, C. Zhao, S. Bullman, A. Bhutkar, B. Hu, S. Ameh, D. Sandel, X. S. Liang, S. Mazzilli, M. T. Whary, M. Meyerson, R. Germain, P. C. Blainey, J. G. Fox, T. Jacks, Commensal Microbiota Promote Lung Cancer Development via γδ T Cells, *Cell* , 998–1013 (2019).

56. F. McAllister, J. Bailey, J. Alsina, C. Nirschl, R. Sharma, H. Fan, Y. Rattigan, J. C. C. Roeser, R. H. H. Lankapalli, H. Zhang, E. M. M. Jaffee, C. G. G. Drake, F. Housseau, A. Maitra, J. K. K. Kolls, C. L. L. Sears, D. M. M. Pardoll, S. D. D. Leach, Oncogenic Kras Activates a Hematopoietic-to-Epithelial IL-17 Signaling Axis in Preinvasive Pancreatic Neoplasia, *Cancer Cell* **25**, 621–637 (2014).

57. T. R. Kress, A. Sabò, B. Amati, MYC: connecting selective transcriptional control to global RNA production., *Nat. Rev. Cancer* **15**, 593–607 (2015).

58. N. Kiuchi, K. Nakajima, M. Ichiba, T. Fukada, M. Narimatsu, K. Mizuno, M. Hibi, T. Hirano, STAT3 Is Required for the gp130-mediated Full Activation of the c- myc Gene, *J. Exp. Med.* **189**, 63–73 (1999).

59. T. Bowman, M. A. Broome, D. Sinibaldi, W. Wharton, W. J. Pledger, J. M. Sedivy, R. Irby, T. Yeatman, S. A. Courtneidge, R. Jove, Stat3-mediated Myc expression is required for Src transformation and PDGF-induced mitogenesis, *Proc. Natl. Acad. Sci.* **98**, 7319–7324 (2001).

60. R. Sears, G. Leone, J. DeGregori, J. R. Nevins, Ras enhances Myc protein stability, *Mol. Cell* **3**, 169–179 (1999).

61. R. Sears, Multiple Ras-dependent phosphorylation pathways regulate Myc protein stability, *Genes Dev.* **14**, 2501–2514 (2000).

Tables

Table 1. Univariate Coxph survival analysis of stage II/III CRC patients in discovery (GSE39582), verification (PETACC3), and combined cohorts based on *IL22RA1* and *KRAS* mutation status.

	RFS				OS			
	No.	*P*	HR	95% CI	No.	*P*	HR	95% CI
GSE39582								
IL22RA1^{high} / IL22RA1^{low}	149 / 288	0.1700	0.77	0.54 to 1.12	150 / 292	0.3330	0.84	0.59 to 1.19
KRAS mut / KRAS WT	163 / 274	**0.0103**	**1.57**	**1.11 to 2.23**	165 / 277	0.0533	1.40	1.00 to 1.96
Within IL22RA1^{low}: KRAS mut / KRAS WT	115 / 173	0.4840	1.16	0.76 to 1.78	117 / 175	0.8130	1.05	0.69 to 1.61
Within IL22RA1^{high}: KRAS mut / KRAS WT	48 / 101	**0.0006**	**2.93**	**1.59 to 5.43**	48 / 102	**0.0023**	**2.45**	**1.38 to 4.36**
Within KRAS WT: IL22RA1^{high} / IL22RA1^{low}	101 / 173	**0.0365**	**0.57**	**0.34 to 0.97**	102 / 175	0.0650	0.64	0.40 to 1.03
Within KRAS mut: IL22RA1^{high} / IL22RA1^{low}	48 / 115	0.1860	1.43	0.84 to 2.42	48 / 115	0.1930	1.43	0.84 to 2.43
PETACC3								
IL22RA1^{high} / IL22RA1^{low}	217 / 429	0.4160	1.11	0.86 to 1.43	217 / 429	0.7300	0.95	0.70 to 1.28
KRAS mut / KRAS WT	254 / 392	**0.0215**	**1.34**	**1.04 to 1.72**	254 / 392	**0.0051**	**1.51**	**1.13 to 2.02**
Within IL22RA1^{low}: KRAS mut / KRAS WT	175 / 254	0.2660	1.19	0.87 to 1.63	175 / 254	0.1260	1.32	0.92 to 1.88
Within IL22RA1^{high}: KRAS mut / KRAS WT	79 / 138	**0.0149**	**1.68**	**1.11 to 2.56**	79 / 138	**0.0070**	**2.00**	**1.21 to 3.30**
Within KRAS WT: IL22RA1^{high} / IL22RA1^{low}	138 / 254	0.8800	0.97	0.68 to 1.39	138 / 254	0.3890	0.83	0.54 to 1.27
Within KRAS mut: IL22RA1^{high} / IL22RA1^{low}	79 / 175	0.1040	1.38	0.94 to 2.02	79 / 175	0.3670	1.22	0.79 to 1.89
Combined								
IL22RA1^{high} / IL22RA1^{low}	372 / 711	0.9200	0.99	0.83 to 1.19	439 / 879	0.4170	0.93	0.77 to 1.12
KRAS mut / KRAS WT	417 / 666	**0.0006**	**1.43**	**1.16 to 1.75**	481 / 837	**0.0054**	**1.35**	**1.09 to 1.66**
Within IL22RA1^{low}: KRAS mut / KRAS WT	287 / 424	0.1800	1.19	0.92 to 1.53	338 / 541	0.5030	1.09	0.84 to 1.42
Within IL22RA1^{high}: KRAS mut / KRAS WT	130 / 242	**0.0000**	**2.05**	**1.45 to 2.89**	143 / 296	**0.0001**	**2.07**	**1.44 to 2.96**
Within KRAS WT: IL22RA1^{high} / IL22RA1^{low}	242 / 424	0.1390	0.80	0.60 to 1.07	296 / 541	**0.0468**	**0.74**	**0.55 to 1.00**
Within KRAS mut: IL22RA1^{high} / IL22RA1^{low}	130 / 287	**0.0465**	**1.37**	**1.00 to 1.87**	143 / 338	0.0660	1.36	0.98 to 1.89

Table 2. Univariate and multivariate Coxph interaction analysis between mutant KRAS and cytokine receptor expression for stage II, III patients from combined cohort

	RFS			OS		
Univariate	***P***	**HR**	**95% CI**	***P***	**HR**	**95% CI**
IL22RA1 * KRAS mut	**0.0065**	**1.76**	**1.17 to 2.63**	**0.0179**	**1.65**	**1.09 to 2.50**
IL6R * KRAS mut	0.4763	1.16	0.77 to 1.75	0.2205	1.30	0.85 to 1.98
IL17RA * KRAS mut	0.5082	1.15	0.76 to 1.76	0.4399	0.84	0.55 to 1.30
Site * KRAS mut	0.9535	0.99	0.66 to 1.48	0.8421	0.96	0.64 to 1.43
Multivariate (BRAF, MSI status, Gender, Tumor site)						
IL22RA1 * KRAS mut	**0.0031**	**1.89**	**1.24 to 2.89**	0.0640	1.52	0.98 to 2.36
IL6R * KRAS mut	0.6282	1.11	0.73 to 1.70	0.3577	1.23	0.79 to 1.93
IL17RA * KRAS mut	0.7419	1.08	0.69 to 1.68	0.6561	0.90	0.56 to 1.43

Figure Legends:

Figure 1. KRAS mutation confers poor prognosis in stage II/III CRCs expressing high amounts of *IL22RA1*. (**A** to **F**) Kaplan-Meier estimates of relapse free survival (RFS) in stage II/III patients in the GSE39582 cohort based on (**A)** *IL22RA1* expression (**B**) *KRAS* mutation status. RFS among (**C**) *IL22RA1*-high and (**D**) *IL22RA1*-low patients based on *KRAS* mutation status. RFS among *IL22RA1*-high patients with tumors (**E**) proximal or (**F**) distal to the splenic flexure based on *KRAS* mutation status. *IL22RA1*-high and low is defined by a cutpoint at the 67th percentile determined using ROC analysis. *P* values computed using Wald-tests. Hazard ratios (HR) are univariate Cox proportional hazard ratios with 95% confidence intervals for the GSE39582 cohort.

Table 1. *IL22RA1*-high and low is defined by a cutpoint at the 67th percentile determined using Receiver operator characteristic (ROC) analysis in the discovery cohort. This cutpoint was used to define *IL22RA1*-high and low in all downstream analyses. Cox proportional hazard ratios (HR) for relapse free sruvival (RFS) and overall survival (OS) are displayed with 95% confidence intervals (95% CI). Significant results are bolded. Patient number (No.) in each subgroup are indicated.

Table 2. The top tertile for each cytokine receptor gene was classified as "high". Cox proportional hazard ratios (HR) for relapse free survival (RFS) and overall survival (OS) are displayed with 95% confidence intervals (95% CI). Significant interactions are bolded. Covariates included in the multivariate analysis were: BRAF mutation status, microsatellite stability/instability status, gender, and tumor site.

Figure 2. High expression of either or both subunits of the heterodimeric IL-22R confers poor prognosis in stage II/III KRAS mutant colorectal cancer. (**A**) Univariate Cox proportional hazard interaction analyses performed on all cytokines/cytokine receptor genes and *KRAS* mutation status in the combined cohort. The highest expression tertile for each gene was defined as "high". Genes for whom the uncorrected *P* value was less than 0.05 are highlighted in blue (RFS HR < 1) and red (RFS HR > 1). (**B**) RFS among stage II/III patients in the discovery cohort stratified based on both *IL22RA1* and *IL10RB* expression and *KRAS* mutation status. *IL22RA1*-high/low and *IL10RB*-high/low is defined by a cutpoint at the 67th percentile for each gene. 5-year (60 month) relapse free survival proportions for each molecular subtype are displayed. (**C**) Relative proportions of Stage II/III patients in the discovery cohort categorized based on *IL22RA1* expression, *IL10RB* expression, and *KRAS* mutation status. The 5-year survival of each molecular subtype is indicated.

Figure 3. IL-22 augments proliferation in KRAS mutant cells. (**A**) qPCR analysis of *SOCS3* induction in Colo205 (KRAS WT), DLD-1 (KRAS MUT), SW480 (KRAS MUT) CRC cells after 24h IL-22 stimulation (n=3). Statistical significance was determined using two-way ANOVA. (**B**) Proliferation of Colo205, DLD-1, SW480 cells following 24, 48, or 72h IL-22

stimulation assessed by MTT assay. Raw 570nm absorbances were blank corrected and normalized to the mean of the 0ng/mL condition for each cell line and each independent experiment (n=3). Statistical significance was determined using two-way ANOVA. (**C**) Flow cytometric analysis (quantification and representative histogram [grey = isotype control staining]) of IL-22RA1 protein (n=5) and (**D**) qPCR analysis of *IL22RA1* mRNA (n=3) at baseline in a DLD-1 isogenic cell line harboring an endogenous *KRAS* G13D mutation in the parental line (KRAS MUT) that is deleted in the partner line (KRAS WT). Statistical significance evaluated using unpaired T-tests. (**E** to **F**) Intracellular flow cytometric analysis of pERK1/2 or pSTAT3-Y705 in KRAS MUT or WT DLD-1 isogenic cells stimulated for 30 minutes with IL-22 (n=4). Data are fold change in MFI over the MFI of the 0ng/mL condition in the KRAS WT line for each independent experiment. (**G**) qPCR analysis of *SOCS3* induction in DLD-1 isogenic cells after 24h IL-22 stimulation (n=3). For dose response experiments, statistical significance was determined using multiple unpaired T-test comparing the KRAS MUT to WT line at each IL-22 dose (**P*<0.05). (**H, I**) Proliferation of DLD-1 KRAS MUT or WT isogenic cells following 24, 48, or 72h IL-22 or IL-6 stimulation assessed by MTT assay. Raw 570nm absorbances were blank corrected and normalized to the mean of the 0ng/mL condition for each cell line and each independent experiment (n=4 [IL-22], n=3 [IL-6]). Statistical significance was determined using a two-way ANOVA and Sidak method to correct for multiple comparisons (**P*<0.0323, ***P*<0.0021, ****P*<0.0002, *****P*<0.0001). (**J**) Representative confocal microscopic images of pSTAT3-Y705 induction in primary CRC organoids stimulated for 30 minutes with 1ng/mL IL-22. (**K**) Proliferation of KRAS MUT (N=3 [N=2 KRAS G12D, N=1 KRAS G12V]) and WT (N=5) organoids treated with 1ng/mL IL-22 for 96h, assessed by Alamar Blue assay. Data are normalized to the NT condition for each line; each data point is the average of 3 technical replicates. Statistical significance was assessed using

unpaired T-tests. All data are mean ± SEM. MFI, mean fluorescence intensity; iso, isotype control; O.D., optical density; NT, no treatment

Figure 4. Mutant KRAS enhances IL-22 induced expression of c-Myc and its downstream targets. (**A**) Experimental workflow for RNA-sequencing analysis. DLD-1 KRAS MUT or WT isogenic cells were stimulated for 2h or 24h with 10ng/mL IL-22 or 10ng/mL IL-6. RNA-sequencing was performed on the 2h and 24h samples. 3 independent experiments were performed. (**B**) Principal component analysis on all samples (n=36). (**C**) Interaction analysis of single sample GSEA analysis (ssGSEA) scores to identify pathways uniquely regulated by IL-22 in KRAS MUT cells. Heatmap represents ssGSEA scores for each sample and displays only the significantly differentially regulated pathways (*P* adjusted < 0.01). (**D**) *MYC* expression following 2h IL-22 stimulation in DLD-1 isogenic cells. N=3 independent experiments. Statistical significance was assessed using unpaired T-tests. (**E**) Expression of genes in "MYC_TARGETS_V2" MSigDB Hallmark signature in 24h IL-22 stimulated DLD-1 isogenic cells. Heatmap represents row normalized log2(PRKM+1) values. (**F**) Total c-Myc expression in DLD-1 KRAS MUT or WT isogenic cells stimulated with 10ng/mL IL-22 for 15 minutes (15") to 24h (24') assessed by Western blot. Blot representative of n=3 independent experiments. (**G**) Proliferation of DLD-1 KRAS MUT and WT cells in response to 48h 10ng/mL IL-22 treatment following 48h *MYC* siRNA knockdown, assessed by MTT assay. Data are blank corrected 570nm absorbances normalized to the MUT siscr NT condition for each independent experiment (n=4-9). Statistical significance was assessed using unpaired T-tests. NT, no treatment; PC, principal component; FDR, false discovery rate; siscr, cells transfected with non-targeting control siRNA; siMYC, cells transfected with *MYC* siRNA

Figure 1.

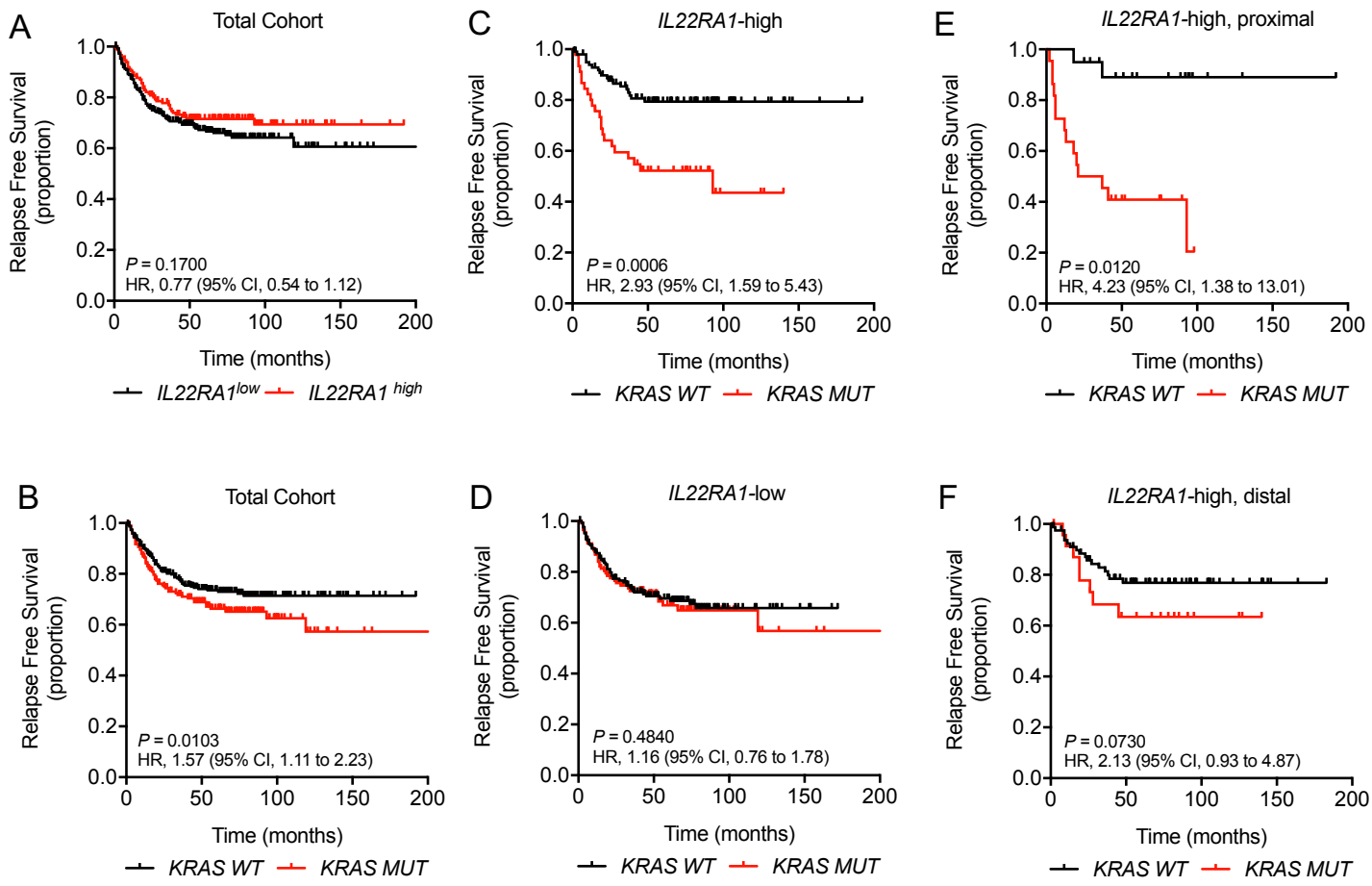
A
Total Cohort
Relapse Free Survival (proportion)
P = 0.1700
HR, 0.77 (95% CI, 0.54 to 1.12)
Time (months)
IL22RA1low
IL22RA1 high
C
IL22RA1-high
P = 0.0006
HR, 2.93 (95% CI, 1.59 to 5.43)
KRAS WT
KRAS MUT
E
IL22RA1-high, proximal
P = 0.0120
HR, 4.23 (95% CI, 1.38 to 13.01)
B
Total Cohort
P = 0.0103
HR, 1.57 (95% CI, 1.11 to 2.23)
D
IL22RA1-low
P = 0.4840
HR, 1.16 (95% CI, 0.76 to 1.78)
F
IL22RA1-high, distal
P = 0.0730
HR, 2.13 (95% CI, 0.93 to 4.87)

Figure 2.

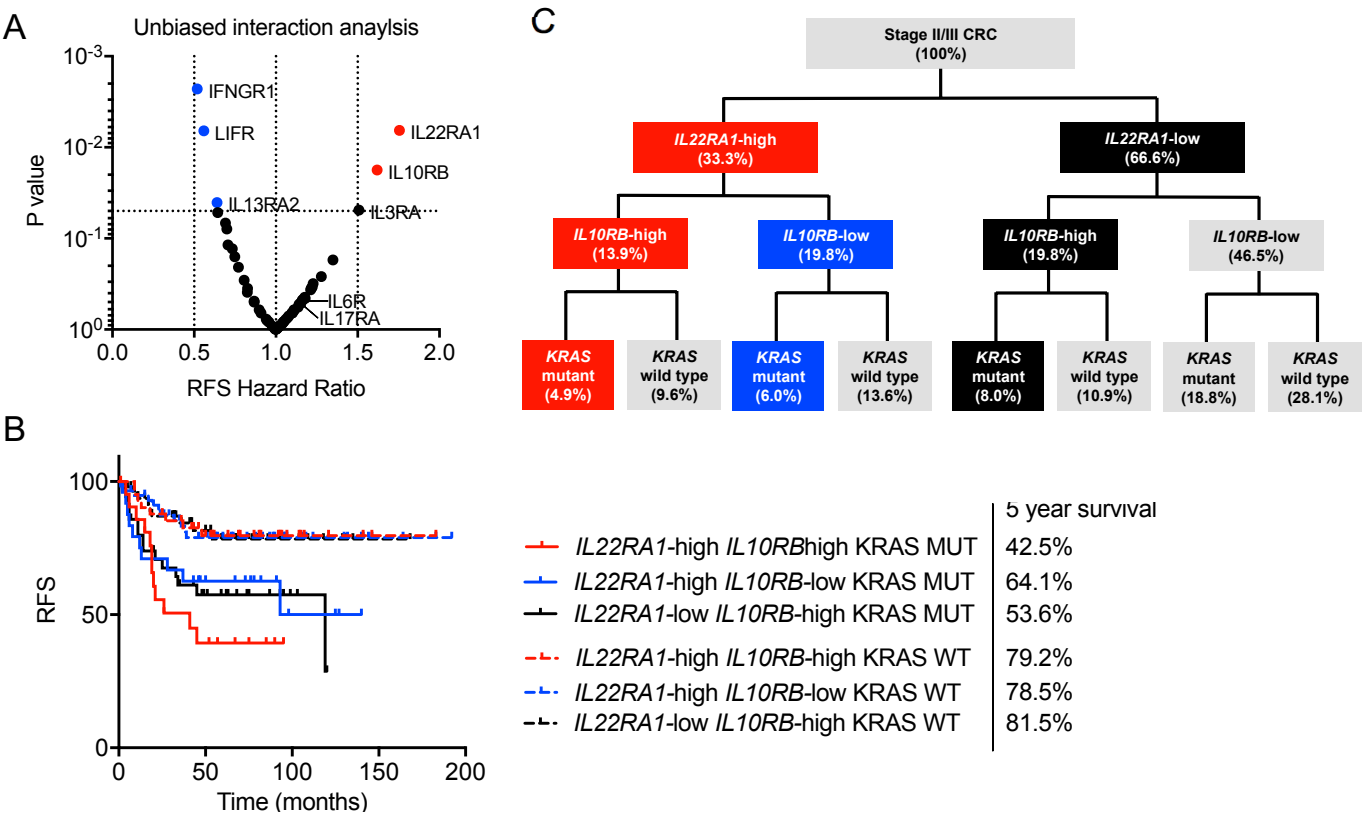
A
Unbiased interaction anaylsis
P value
RFS Hazard Ratio
IFNGR1
LIFR
IL22RA1
IL10RB
IL13RA2
IL3RA
IL6R
IL17RA
B
RFS
Time (months)
C
Stage II/III CRC (100%)
IL22RA1-high (33.3%)
IL22RA1-low (66.6%)
IL10RB-high (13.9%)
IL10RB-low (19.8%)
IL10RB-high (19.8%)
IL10RB-low (46.5%)
KRAS mutant (4.9%)
KRAS wild type (9.6%)
KRAS mutant (6.0%)
KRAS wild type (13.6%)
KRAS mutant (8.0%)
KRAS wild type (10.9%)
KRAS mutant (18.8%)
KRAS wild type (28.1%)
5 year survival
IL22RA1-high IL10RBhigh KRAS MUT 42.5%
IL22RA1-high IL10RB-low KRAS MUT 64.1%
IL22RA1-low IL10RB-high KRAS MUT 53.6%
IL22RA1-high IL10RB-high KRAS WT 79.2%
IL22RA1-high IL10RB-low KRAS WT 78.5%
IL22RA1-low IL10RB-high KRAS WT 81.5%

Figure 3.

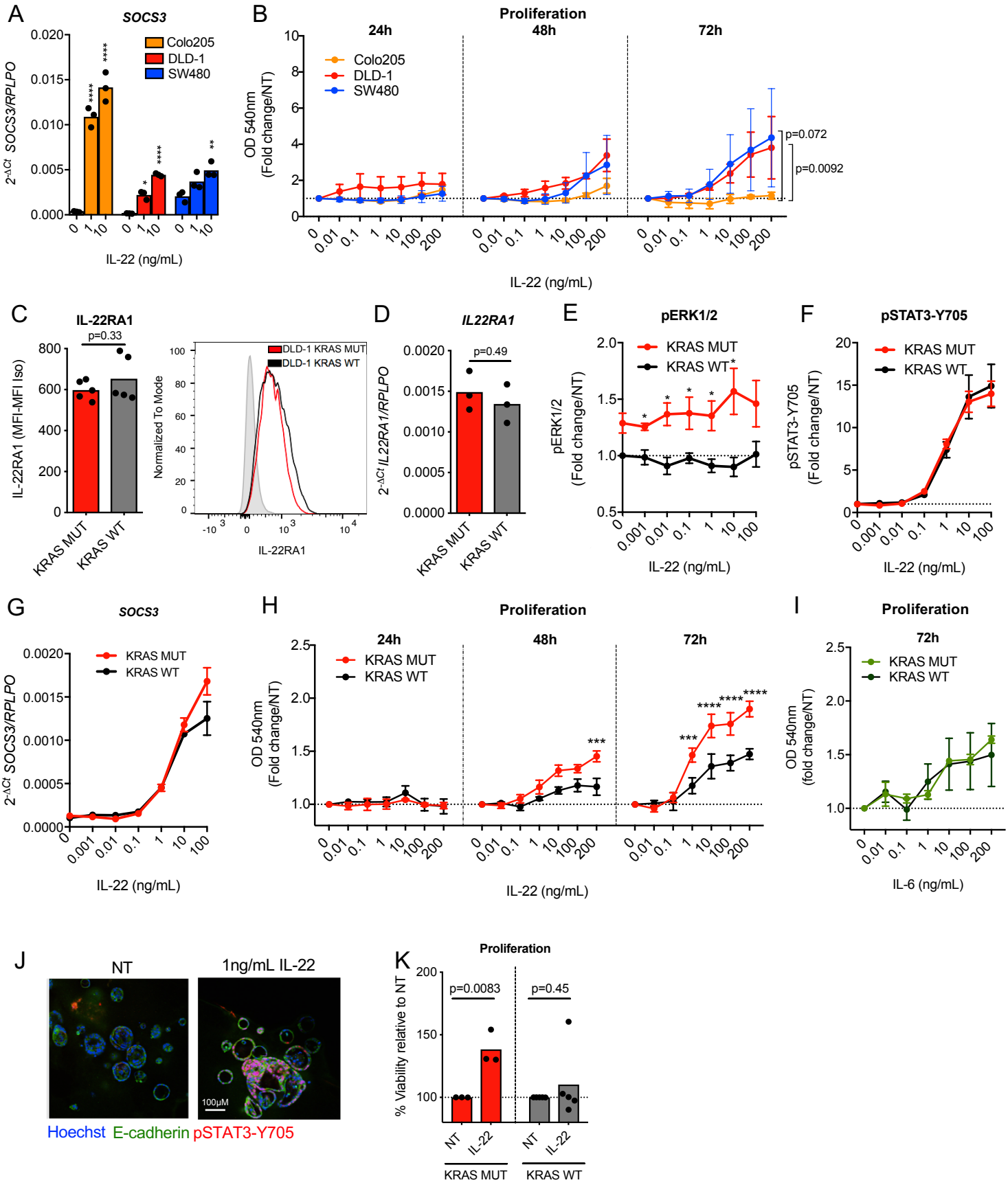
A
SOCS3
2^-ΔCt SOCS3/RPLPO
Colo205
DLD-1
SW480
IL-22 (ng/mL)
B
Proliferation
24h
48h
72h
OD 540nm (Fold change/NT)
p=0.072
p=0.0092
IL-22 (ng/mL)
C
IL-22RA1
p=0.33
IL-22RA1 (MFI-MFI Iso)
KRAS MUT
KRAS WT
DLD-1 KRAS MUT
DLD-1 KRAS WT
Normalized To Mode
IL-22RA1
D
IL22RA1
p=0.49
2^-ΔCt IL22RA1/RPLPO
E
pERK1/2
pERK1/2 (Fold change/NT)
IL-22 (ng/mL)
F
pSTAT3-Y705
pSTAT3-Y705 (Fold change/NT)
IL-22 (ng/mL)
G
SOCS3
2^-ΔCt SOCS3/RPLPO
IL-22 (ng/mL)
H
Proliferation
OD 540nm (Fold change/NT)
IL-22 (ng/mL)
I
Proliferation
72h
OD 540nm (fold change/NT)
IL-6 (ng/mL)
J
NT
1ng/mL IL-22
100μM
Hoechst E-cadherin pSTAT3-Y705
K
Proliferation
% Viability relative to NT
p=0.0083
p=0.45
NT
IL-22
KRAS MUT
KRAS WT

Figure 4.

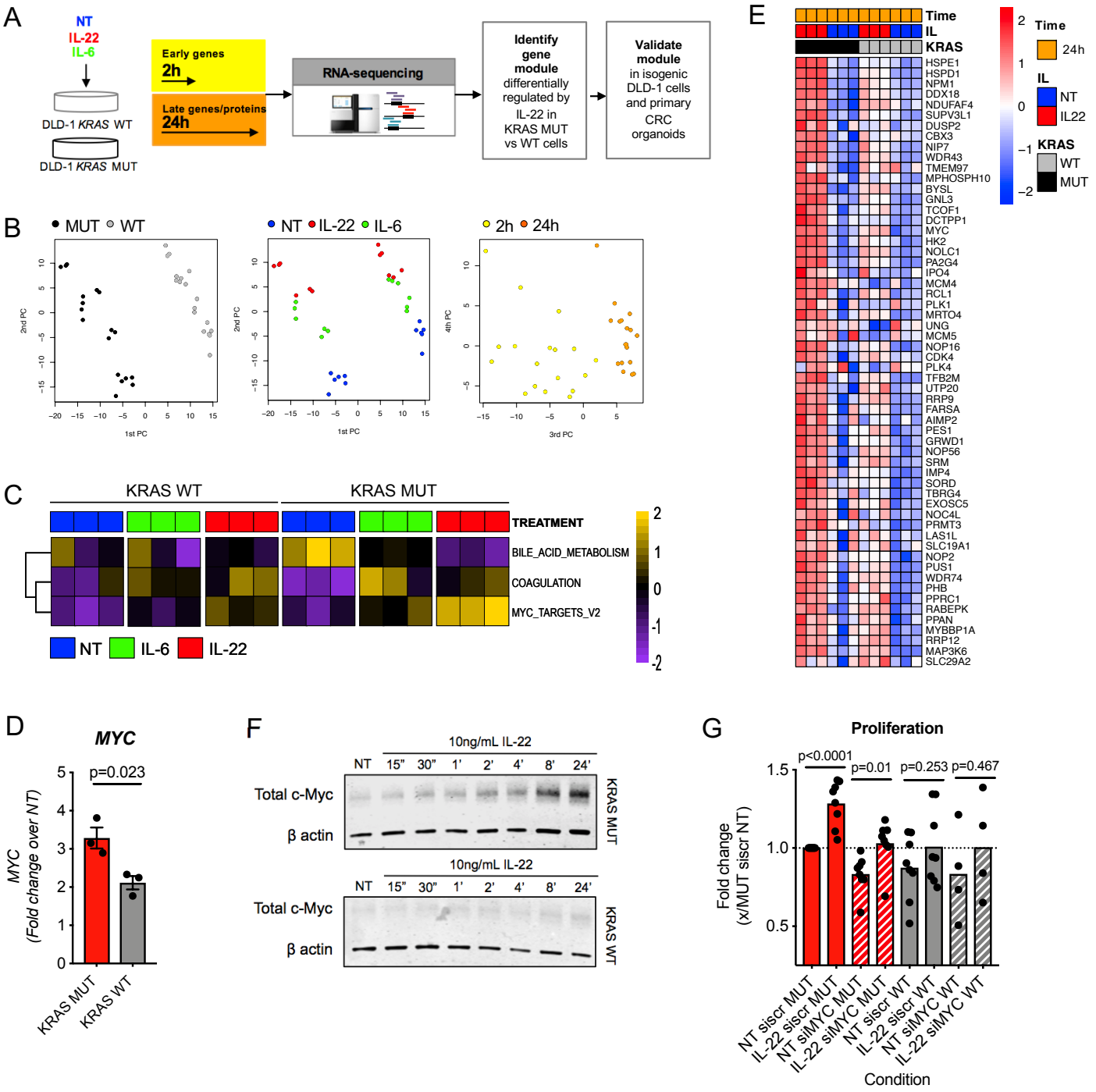
A
NT
IL-22
IL-6
DLD-1 KRAS WT
DLD-1 KRAS MUT
Early genes
2h
Late genes/proteins
24h
RNA-sequencing
Identify gene module differentially regulated by IL-22 in KRAS MUT vs WT cells
Validate module in isogenic DLD-1 cells and primary CRC organoids
B
MUT WT
NT IL-22 IL-6
2h 24h
1st PC
2nd PC
3rd PC
4th PC
C
KRAS WT
KRAS MUT
TREATMENT
BILE_ACID_METABOLISM
COAGULATION
MYC_TARGETS_V2
NT IL-6 IL-22
E
Time
IL
KRAS
HSPE1
HSPD1
NPM1
DDX18
NDUFAF4
SUPV3L1
DUSP2
CBX3
NIP7
WDR43
TMEM97
MPHOSPH10
BYSL
GNL3
TCOF1
DCTPP1
MYC
HK2
NOLC1
PA2G4
IPO4
MCM4
RCL1
PLK1
MRTO4
UNG
MCM5
NOP16
CDK4
PLK4
TFB2M
UTP20
RRP9
FARSA
AIMP2
PES1
GRWD1
NOP56
SRM
IMP4
SORD
TBRG4
EXOSC5
NOC4L
PRMT3
LAS1L
SLC19A1
NOP2
PUS1
WDR74
PHB
PPRC1
RABEPK
PPAN
MYBBP1A
RRP12
MAP3K6
SLC29A2
24h
NT
IL22
WT
MUT
D
MYC
p=0.023
MYC (Fold change over NT)
KRAS MUT
KRAS WT
F
10ng/mL IL-22
NT 15" 30" 1' 2' 4' 8' 24'
Total c-Myc
β actin
KRAS MUT
KRAS WT
G
Proliferation
p<0.0001
p=0.01
p=0.253
p=0.467
Fold change (x/MUT siscr NT)
NT siscr MUT
IL-22 siscr MUT
NT siMYC MUT
IL-22 siMYC MUT
NT siscr WT
IL-22 siscr WT
NT siMYC WT
IL-22 siMYC WT
Condition